Information Sciences 568 (2021) 403–426

Contents lists available at ScienceDirect

Information Sciences

journal homepage: www.elsevier.com/locate/ins

Bilingual autoencoder-based efficient harmonization of multi-source private data for accurate predictive modeling

Taek-Ho Lee [a], Junghye Lee [b,*], Chi-Hyuck Jun [a,*]

[a] Department of Industrial and Management Engineering, Pohang University of Science and Technology (POSTECH), 77 Cheongam-Ro, Pohang 37673, Republic of Korea

[b] Department of Industrial Engineering, Ulsan National Institute of Science and Technology (UNIST), 50 UNIST-gil, Ulsan 44919, Republic of Korea

ARTICLE INFO

Article history:
Received 15 September 2020
Received in revised form 25 March 2021
Accepted 29 March 2021
Available online 06 April 2021

Keywords:
Distributed EHR
Contextual embedding
Space alignment
Autoencoder
Predictive tasks

ABSTRACT

Sharing electronic health record data is essential for advanced analysis, but may put sensitive information at risk. Several studies have attempted to address this risk using contextual embedding, but with many hospitals involved, they are often inefficient and inflexible. Thus, we propose a bilingual autoencoder-based model to harmonize local embeddings in different spaces. Cross-hospital reconstruction of embeddings makes encoders map embeddings from hospitals to a shared space and align them spontaneously. We also suggest two-phase training to prevent distortion of embeddings during harmonization with hospitals that have biased information. In experiments, we used medical event sequences from the Medical Information Mart for Intensive Care-III dataset and simulated the situation of multiple hospitals. For evaluation, we measured the alignment of events from different hospitals and the prediction accuracy of a patient's diagnosis in the next admission in three scenarios in which local embeddings do not work. The proposed method efficiently harmonizes embeddings in different spaces, increases prediction accuracy, and gives flexibility to include new hospitals, so is superior to previous methods in most cases. It will be useful in predictive tasks to utilize distributed data while preserving private information.

1. Introduction

Machine learning and artificial intelligence (AI) are increasingly used in healthcare [23]. Many hospitals have adopted electronic health record (EHR) systems since the Health Information Technology for Economic and Clinical Health (HITECH) Act of 2009 [43], so a large amount of medical data has been collected. Many studies have analyzed these medical data to assist in medical diagnosis [26], information extraction [33], and cost reduction [24]. Many attempts have also been made to apply deep-learning techniques in medical informatics [23,43,46]. However, the amount of data stored in an individual institution (i.e., hospital) may be insufficient to learn a predictive AI model [9]; furthermore, data from one hospital may show bias, so a model trained on them may not be generalizable to patients in another hospital, and this inability is a major challenge in healthcare [46].

Learning of generalizable models requires use of combined EHR data from several hospitals. However, sharing of EHR data risks breach of confidentiality, so strict regulations, such as the Health Insurance Portability and Accountability Act (HIPAA) in United States [37], the California Consumer Privacy Act of 2018 (CCPA) [4], and the EU General Data Protection Regulation

* Corresponding authors.
E-mail addresses: taekho.lee@potsech.ac.kr (T.-H. Lee), junghyelee@unist.ac.kr (J. Lee), chjun@postech.ac.kr (C.-H. Jun).

https://doi.org/10.1016/j.ins.2021.03.064
0020-0255/

(GDPR) [45], forbid direct sharing of data from multiple institutions [29]. Data can be anonymized to be shared, but most become expensive as the volume of the data increases [47], and confidential information can be inferred even in anonymized data [38].

An alternative to removing identifiable information is to train models on data that are distributed across multiple sources without sharing raw data. Most of these studies assume horizontally distributed data and use traditional predictive models such as naïve Bayes [15], *k*-nearest neighbors [48], support vector machines (SVM) [30], logistic regression [21], ridge regression [7], random forest [32], and neural networks (NNs) [34,31]. Other studies have also analyzed vertically partitioned data using traditional models such as SVM [30] and logistic regression [28]. Most of these methods only share intermediate statistics, such as gradients, but can still reveal sensitive information by the shared statistics [35,49], so they have used privacy and security techniques such as differential privacy (DP) [1,13,21], homomorphic encryption (HE) [7,15,22,25,32,48], and secure multi-party computation (MPC) [7,31]. Despite success in preserving privacy, these techniques cause computational burden and entail a trade-off between privacy and model accuracy. Also, the assumption that distributed datasets can be integrated horizontally or vertically may be unrealistic in some cases.

Some studies construct a predictive model in an environment in which the before-mentioned assumptions are inappropriate such as healthcare. Several studies have recently shown that contextual embeddings of medical events, which are dense and low-dimensional representations learned using NNs, are useful [8,10]. The contextual embeddings contain only relationships among medical events, and do not include patient-level information, so sharing embeddings does not violate privacy, and as a result does not require privacy and security techniques. However, NN algorithms include randomness, so the embeddings learned in each institution lie in independent spaces. This status complicates the task of combining the embeddings from various institutions.

To solve this problem, a variant of noise-contrastive estimation [29] trains the global embedding model by sequentially learning each data source in a way similar to online Word2Vec [36]. This method requires the vocabularies and their frequencies are shared and integrated, but sharing medical events and their frequencies can expose patients' records, so clustering of vocabularies and DP techniques must be used to protect privacy. Including data from new hospitals is also difficult after training. As an alternative, different embedding models can be harmonized by solving the space alignment problem [11,17]. However, this method uses Procrustes [16], a linear transformation between two sets of embeddings at a time, so it requires holding one hospital as the base space, and restricts information used in harmonization.

In this paper, we aim to propose a method for efficient harmonization of embedding models, and this method allows privacy-preserving predictive analysis across multiple institutions while solving the limitations of the previous work. The main contributions of this work are as follows.

- A bilingual autoencoder-based method to harmonize contextual embeddings that have been trained independently from different sources: The proposed method transforms embeddings in separate spaces into embeddings in one space shared by all sources, so transformed embeddings can collaborate in the privacy-preserving predictive analysis. The proposed method can exploit corresponding information from all pairs of sources at once, so it finds the shared space that is most useful, efficiently. This approach significantly improves prediction accuracies in situations that local embeddings alone cannot handle successfully.
- Two-phase training to guide the proposed method to better harmonization even when the size of the sources to be federated differs: This method improves prediction accuracies in both large and small sources by conserving the contextual information of the large sources in the harmonization process, and motivates large ones to participate in the federation.
- Extensive experiments on various scenarios to demonstrate that the alignment and prediction accuracies are superior to those of the previous method, usually significantly.

The rest of this paper is organized as follows. Section 2 explains the predictive procedure, then introduces the structure of the proposed autoencoder and the two-phase training method. Section 3 describes experiments to evaluate the proposed method. This section shows the alignment of the embeddings from different hospitals after harmonization, and the prediction accuracies in three simulation scenarios. Section 4 presents contributions and limitations of this study and provides directions of future work. Section 5 summarizes results of experiments and concludes.

2. Methods

2.1. Preliminaries

Here we outline the concept of predictive modeling before explaining the proposed harmonization method. EHR data include various information such as demographics, clinical notes, and radiological images [43]. A structured part of EHR contains information from diverse clinical aspects such as lab tests, prescriptions, symptoms, conditions, and diagnoses. The temporal clinical pathway of a patient is constructed by listing medical codes of EHR in chronological order. By learning contextual embeddings from constructed clinical pathways, medical events and patients are represented as continuous vectors. To learn contextual embeddings, Word2Vec is used, but other methods such as GloVe [39] or BERT [12] could also be used. After the contextual embeddings are learned, the patient-diagnosis projection similarity (PDPS) method [14] is used to pre-

dict a patient's diagnoses in the next admission. In PDPS, the probability of diagnosis is computed using the cosine similarity between a patient vector and a diagnosis vector. Here, the patient vector means the context vector that encodes information of all medical events in his or her clinical pathway, and is calculated by normalizing the summation of vectors of medical events in the patient's clinical pathway, with each vector weighted by a time-decaying factor.

The overall prediction procedure uses information from multiple hospitals. We present an example that considers two hospitals (Fig. 1). In step 1, each hospital learns local contextual embeddings by using only clinical pathways of its own patients. Contextual embeddings from different hospitals were previously used only in each hospital because they lie in different spaces. In step 2, the harmonization places them in the same space (green box, Fig. 1). In step 3, the harmonized embeddings can be used together in various ways, and PDPS is applied on top of the harmonized embeddings to improve the prediction accuracy. The harmonization method is explained in the next section.

2.2. Bilingual autoencoder

An autoencoder is a multi-layer neural network that consists of two sub-networks: an encoder and a decoder [5]. The encoder transforms its input into latent features; the decoder produces a reconstruction of the input from these latent features. The encoder and decoder are also networks that can have multiple layers. The autoencoder is trained to minimize the reconstruction error, which is

$$L_{AE}(\Theta_{Enc}, \Theta_{Dec}) = \frac{1}{|\boldsymbol{X}|}\sum_{i=1}^{|\boldsymbol{X}|}\|\boldsymbol{x}_i - Dec(Enc(\boldsymbol{x}_i, \Theta_{Enc}), \Theta_{Dec})\|_2^2 \tag{1}$$

where $\boldsymbol{X} \in \mathbb{R}^{|\boldsymbol{X}|\times d_{\boldsymbol{X}}}$ is the input matrix, $|\boldsymbol{X}|$ is the number of instances in X, and $\boldsymbol{x}_i$ is the i-th instance of $\boldsymbol{X}$. Enc and Dec represent the encoder and decoder with parameters Θ_{Enc} and Θ_{Dec}, respectively. In almost all cases, the true objective of the autoencoder is not just to copy the original input but to learn representations that take useful properties as an output of the encoder

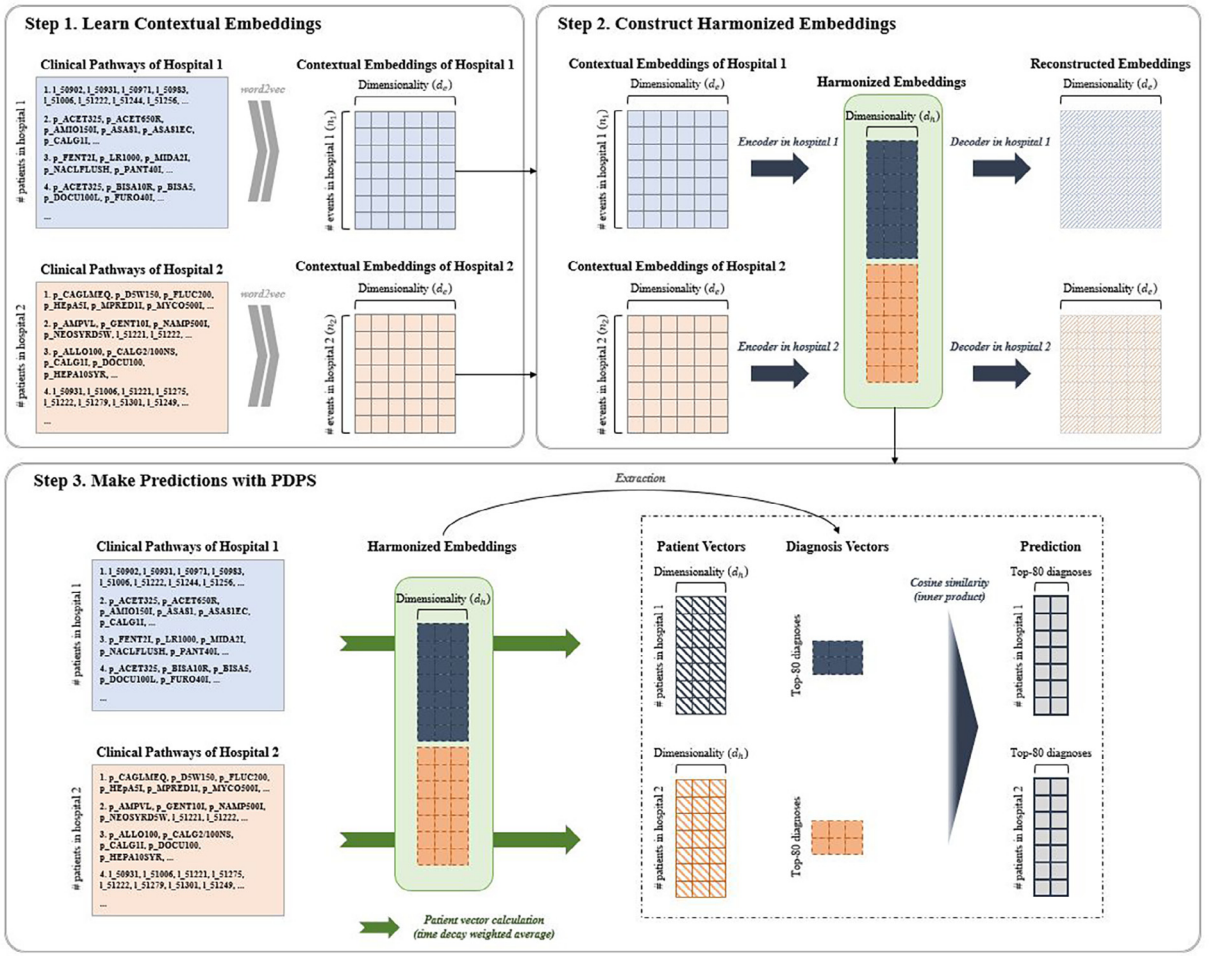

Fig. 1. The overall procedure of prediction. Details are provided in the text.

(i.e., bottleneck layer). The last layer of the encoder usually has smaller dimensionality than the input layer to prevent the autoencoder from learning a trivial copy of the input. In addition to limiting the number of dimensions in the bottleneck layer, many recent studies on autoencoders have developed various strategies to learn useful information about the input data [6,41]. The representations learned by these autoencoders have proven their usefulness in various tasks such as image generation [40] and recommendation systems [27].

Also in natural language processing, bilingual autoencoder models are proposed to learn hidden representations by extracting information from both languages [42]. Suppose that we have a set of (m, n) pairs where m and n are each a bag-of-words that indicate the same sentence in languages M and N, respectively. To learn similar representations for pairs, an autoencoder is forced to reconstruct the bag-of-words in both languages from the sentence in either language. For cross-lingual reconstruction, distinct encoders and decoders are trained for each language. Encoders map the sentence in the form of a bag-of-words into the shared continuous space, and decoders can reconstruct the sentence given a representation from either language. To train overall encoders and decoders simultaneously, four loss functions are defined according to which language is reconstructed from which language. Some variations of the bilingual autoencoder have been proposed with technical improvement, but their structures are mostly as described above [3,44].

2.3. Harmonization model derived from bilingual autoencoder

Inspired by the bilingual autoencoder, we propose HarmoAE (Fig. 2), which is an autoencoder model to harmonize embeddings from multiple sources (i.e., hospitals). As in the bilingual autoencoder [3,42], the encoder and decoder are trained for each hospital independently. We make decoders reconstruct the embeddings by using hidden representations from any hospital, and encoders map embeddings in each hospital into a hidden space that is shared by all hospitals. In reality, hospitals may use different terminologies even for the same medical events. Therefore, only some event pairs that are known to be the same in two hospitals, such as International Classification of Diseases (ICD), can be used to train encoder and decoder in different hospitals. These event pairs are called corresponding pairs. After all encoders and decoders are trained, all embeddings from hospitals are mapped into a common hidden space and can be used as harmonized embeddings.

Suppose a set of k hospitals, each of which has contextual embeddings with dimensionality d_e. Let $\boldsymbol{X}_i \in \mathbb{R}^{n_i \times d_e}$ be an embedding matrix of hospital i where n_i is the number of medical events in hospital i. Let $\boldsymbol{H}_i$ be hidden representations with dimensionality d_h encoded from the hospital i. Then, for $i = 1, \ldots, k$, the encoding is

$$\boldsymbol{H}_i = Enc_i(\boldsymbol{X}_i) = f_a(\boldsymbol{X}_i \boldsymbol{W}_i + \mathbf{1}_{n_i} \cdot \boldsymbol{b}_i^T) \tag{2}$$

where $\boldsymbol{W}_i \in \mathbb{R}^{d_e \times d_h}$ and $\boldsymbol{b}_i \in \mathbb{R}^{d_h}$ represent respectively the weights and bias for the encoder of hospital i and f_a is the activation function of a hidden layer. $\mathbf{1}_{n_i} \in \mathbb{R}^{n_i}$ is an n_i-dimensional vector in which all elements are 1. In the notation $\boldsymbol{H}_i$, the subscript i clarifies where the hidden representations come from although they need not be distinguished in the harmonized embeddings. Each $\boldsymbol{H}_i$ can be mapped to the embedding space of any hospital.

Let $\boldsymbol{Y}_{i,j}$ be the reconstructed embedding matrix in hospital j given the hidden representation $\boldsymbol{H}_i$ from the embedding matrix $\boldsymbol{X}_i$ in hospital i. Then, for $i = 1, \ldots, k$ and $j = 1, \ldots, k$, the decoding is

$$\boldsymbol{Y}_{i,j} = Dec_j(\boldsymbol{H}_i) = f_a^{linear}(\boldsymbol{H}_i \boldsymbol{V}_j + \mathbf{1}_{n_i} \cdot \boldsymbol{c}_j^T) \tag{3}$$

where $\boldsymbol{V}_j \in \mathbb{R}^{d_h \times d_e}$ and $\boldsymbol{c}_j \in \mathbb{R}^{d_e}$ represent respectively the weights and the bias of the decoder that corresponds to hospital j. Decoders have a linear activation function f_a^{linear} to predict continuous embedding values.

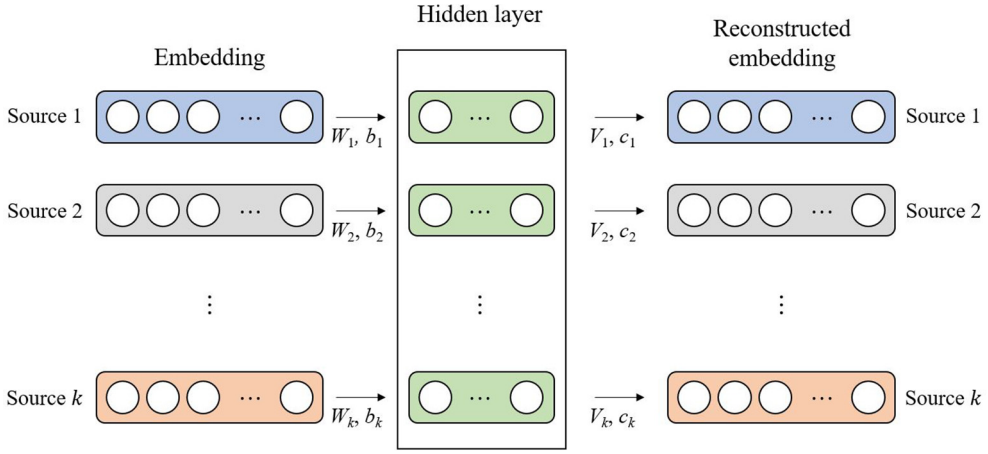

Fig. 2. The structure of HarmoAE. Each color represents one embedding space.

To train HarmoAE we define the loss function as the sum of the averaged reconstruction errors of all hospital pairs. The loss function consists of a total of k^2 terms, of which k terms are self-reconstruction errors and $k(k-1)$ terms are cross-hospital reconstruction errors. The definition of loss function L is

$$L = \sum_{i=1}^{k} L_i^{self} + \sum_{i=1}^{k}\sum_{j=1}^{k} \mathbb{I}(i \neq j) \cdot L_{i,j}^{cross} \tag{4}$$

where L_i^{self} is the average self-reconstruction error of hospital i and $L_{i,j}^{cross}$ is the cross-hospital reconstruction error; both errors are defined below. The indicator $\mathbb{I}(\cdot)$ returns 1 if $\cdot$ is true, and 0 otherwise.

The average self-reconstruction error L_i^{self} of hospital i is defined as in a general autoencoder as

$$L_i^{self} = \frac{1}{n_i} \| \boldsymbol{Y}_{i,i} - \boldsymbol{X}_i \|_F^2 \tag{5}$$

For the cross-hospital reconstruction error, suppose that we make hidden representations by encoding embeddings in hospital i and decode the hidden representations to the embeddings of hospital j. For the same medical events, embeddings reconstructed from hospital i should be similar to the original embeddings in hospital j. Let $\boldsymbol{X}_{i,j} \in \mathbb{R}^{n_{i,j} \times d_e}$ and $\boldsymbol{X}_{j,i} \in \mathbb{R}^{n_{j,i} \times d_e}$ each be the subset of embeddings in hospital i and j, respectively, and both subsets only contain medical events in corresponding pairs between the two hospitals; the number of events in $\boldsymbol{X}_{i,j}$ and $\boldsymbol{X}_{j,i}$, denoted $n_{i,j}$ and $n_{j,i}$ respectively, are the same. If we assume that medical events in $\boldsymbol{X}_{i,j}$ and $\boldsymbol{X}_{j,i}$ are sorted in the same order, the cross-hospital reconstruction error $L_{i,j}^{cross}$, for $i = 1, \ldots, k$ and $j = 1, \ldots, k$, can be calculated as

$$L_{i,j}^{cross} = \frac{1}{n_{i,j}} \| \boldsymbol{Y}_{i,j}^{cp} - \boldsymbol{X}_{j,i} \|_F^2 \tag{6}$$

where $\boldsymbol{Y}_{i,j}^{cp} = Dec_j(Enc_i(\boldsymbol{X}_{i,j}))$ represents the embeddings in hospital j that were reconstructed using $\boldsymbol{X}_{i,j}$ in hospital i, which includes only medical events in corresponding pairs.

All encoders and decoders of the proposed autoencoder are simultaneously trained with the loss function L. However, if some hospitals have insufficient data, they would have biased embeddings. The biased embeddings can corrupt well-trained embeddings during harmonization. To prevent this occurrence, we suggest a two-phase training for HarmoAE (Fig. 3). During the first phase, pre-training is performed only for encoders and decoders of hospitals that have embeddings learned with sufficient data. The number of patients in each hospital could be a good measure to assess whether the hospital's embeddings are well-trained or not. The pre-trained encoders may form a hidden layer that preserves contextual information of useful embeddings. In the second phase, all other encoders and decoders are concurrently trained, while the weights of the pre-trained encoders are frozen. The freeze prevents the pre-trained encoders from being contaminated when they harmonize with other hospitals.

3. Results

3.1. Experimental setting

We used the structured data of Medical Information Mart for Intensive Care-III (MIMIC-III) dataset, which is a freely-accessible clinical-care database [20]. We pre-processed these data as described in the previous work [17]. We reduced

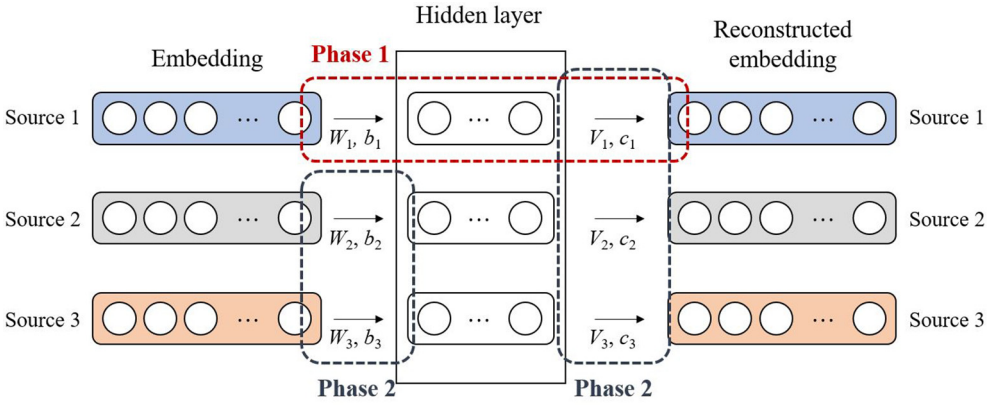

Fig. 3. Illustration of two-phase training for HarmoAE when three hospitals are considered. Here source 1 is a large hospital and sources 2 and 3 are small hospitals.

the ICD codes for diagnoses to three digits, excluded both patients that had one admission and medical events that had fewer than 50 occurrences when we generate patient clinical pathways. Finally, medical event sequences of 5,077 patients for the experiment remained.

We divided these patient sequences into several groups, each of which represents a hospital dataset. We simulated mainly three, four, and five groups, but in one extreme case nine (Appendices A–D). In all cases, we repeated experiments ten times and reported average performance. We used Word2Vec to learn embeddings with each group of patients, and then harmonized the embeddings from different hospitals in the same space by using corresponding pairs. We simulated using one dataset, so hospitals share most terminologies, but this is an unrealistic condition. For the realistic simulation, we allowed each pair of hospitals to randomly select a fraction of events as their corresponding pairs, and so some medical events may belong to corresponding pairs of other hospital pairs. We experimented with several ratios of corresponding pairs, and used different sets of ratios among different experiments. For the parameters of Word2Vec, we set the embedding dimension to 350 and the window size to 30 according to the previous work; whereas, we determined parameters of the proposed method experimentally (Table 1).

We conducted four experiments: One experiment quantified how the harmonization aligns medical events that indicate the same event in different hospitals (Section 3.2), and the other three experiments measured how the harmonization improves prediction accuracy (Section 3.3). In predictive experiments, PDPS predicts the final diagnoses of patients in the test set, given their clinical pathways before final admission. The decay factor used in calculating patient vectors was set to 1.

We compared our method to the previous work [17] that uses Procrustes for harmonization. Procrustes learns a linear mapping that is formulated with an orthogonal matrix and a scaling factor for transformation from one space to another. The optimal transformation is easily computed by singular value decomposition. Here we also used "Global" to describe the contextual embeddings learned with all patients in the training set, and "Local" to embeddings learned with each group of patients; Both embeddings show benchmark performance.

3.2. Alignment

The goal of the embedding harmonization process is to align embeddings from different hospitals by mapping them into the common shared space. After harmonization, distance metrics can directly compare new representations of medical events from different spaces. The alignment measure that uses nearest neighbors quantifies the proximity of pairs of medical events with the same semantics in the aligned space [11]. Given two embedding matrices $\boldsymbol{A}$ and $\boldsymbol{B}$, and a number K of nearest neighbors to search, the measure is defined as the Probability of Capturing the parallel embedding within its Nearest neighbors in the aligned space (PCN). In this paper, we used a slightly modified measure:

$$\mathrm{PCN} = \frac{1}{n_A + n_B}\left\{\sum_{i=1}^{n_A}\mathbb{I}(\boldsymbol{b}_i^f \in N_K(\boldsymbol{a}_i^f, \boldsymbol{B}^f)) + \sum_{j=1}^{n_B}\mathbb{I}(\boldsymbol{a}_j^f \in N_K(\boldsymbol{b}_j^f, \boldsymbol{A}^f)\right\} \tag{7}$$

where $N_K(\boldsymbol{x}, \boldsymbol{X})$ is the set of the K-nearest neighbors of $\boldsymbol{x}$ in a set $\boldsymbol{X}$. $\boldsymbol{A}^f$ and $\boldsymbol{B}^f$ are representations in the aligned space mapped from $\boldsymbol{A}$ and $\boldsymbol{B}$, respectively; $\boldsymbol{a}_i^f$ and $\boldsymbol{b}_i^f$ each is i-th instance of $\boldsymbol{A}^f$ and $\boldsymbol{B}^f$. In this study, because medical events that belong to only one of $\boldsymbol{A}$ and $\boldsymbol{B}$ cannot find parallel embeddings, they are excluded from PCN calculations, so the number of events in $\boldsymbol{A}$ and $\boldsymbol{B}$, denoted n_A and n_B respectively, are the same.

In our experiment, alignment should be measured for multiple spaces. We first calculated PCN for all pairs of spaces and averaged them. Consider three embedding matrices $\boldsymbol{A}, \boldsymbol{B}$, and $\boldsymbol{C}$. Given K, we calculated alignments between $\boldsymbol{A}$ and $\boldsymbol{B}$, $\boldsymbol{B}$ and $\boldsymbol{C}$, $\boldsymbol{C}$ and $\boldsymbol{A}$, then averaged them. We obtained results for the cases of three, four, and five hospitals (Fig. 4). We computed the alignment by adjusting the ratio of corresponding pairs to 40%, 70%, and 100% in a hospital-pairwise perspective; K to 1, 10, 50, and 100. HarmoAE (Encoder Transformed, "EncT") always showed significantly higher average PCN than Procrustes (Procrusted Transformed, "ProT") at the significance level of $p < 0.01$ (paired t-test).

3.3. Prediction

In this section, we measured prediction accuracies in three scenarios in which contextual embeddings trained in each hospital alone cannot provide an accurate prediction. We calculated the area under the receiver operating characteristic

Table 1
Implementation details of HarmoAE.

Item	Value	Item	Value
The number of units in hidden layer	100	Dropout rate (on input and hidden layer)	5%
Optimizer	Adam	Learning rate (initial)	0.001
Activation function	ELU	The number of epochs	500

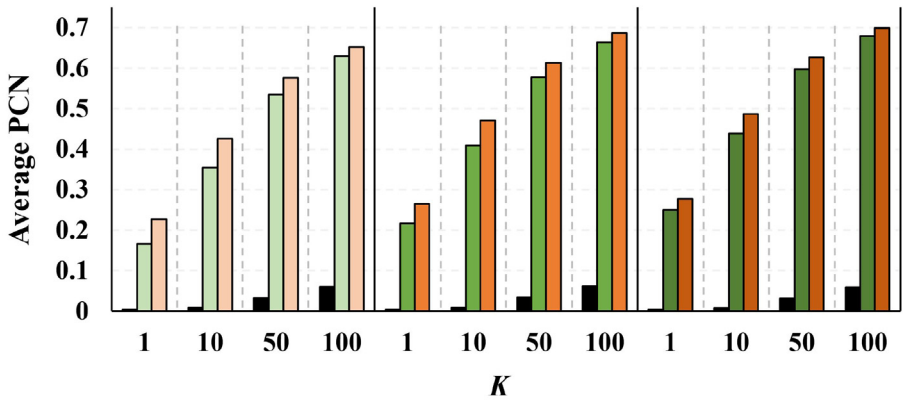

(a) 3 hospitals.

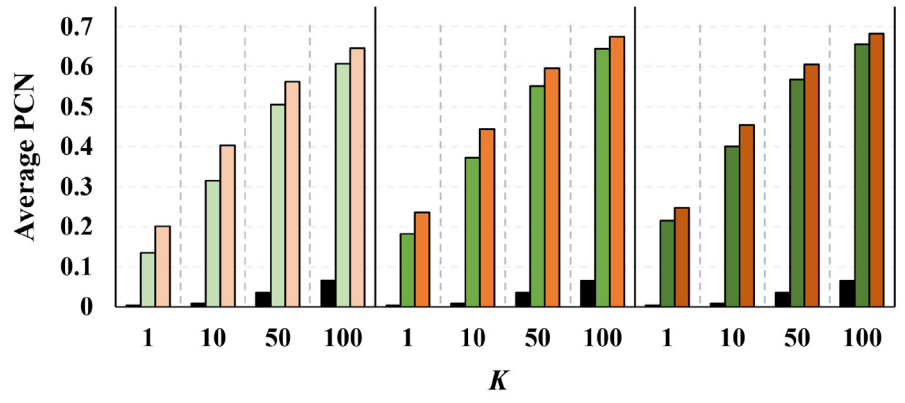

(b) 4 hospitals.

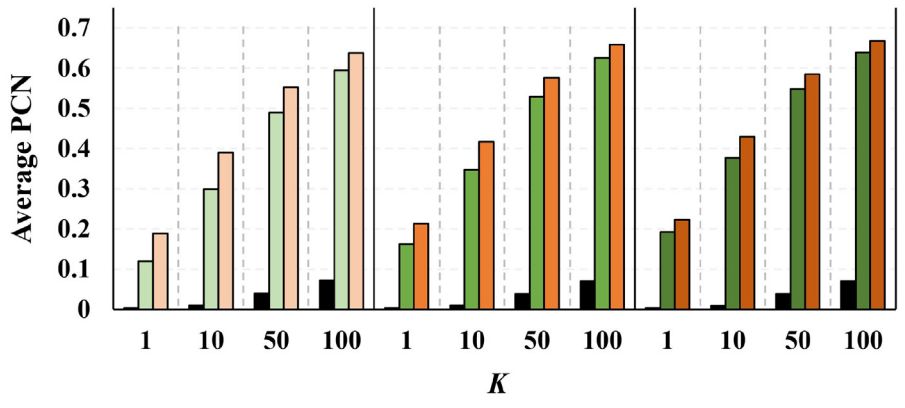

(c) 5 hospitals.

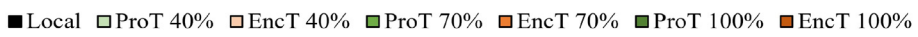

Fig. 4. Average PCN.

curve (AUC) for each of the most common 80 diagnoses (Appendix E) and then averaged them. We selected 500 of 5,077 patients randomly as a test set, and divided patients in the training set into several groups depending on the number of hospitals. In each subsection, we described each scenario in detail.

3.3.1. Incomplete information

Most hospitals may not encounter all possible medical events. Hospitals cannot learn embeddings for missing events, and therefore hospitals cannot predict diagnoses missing at each hospital. However, the harmonized embeddings of the same events from another hospital can compensate for information of the missing events. To simulate hospitals that have missed some diagnoses, we divided the most common 80 diagnoses into k groups, assigned one such group of diagnoses to each hospital, and then for each hospital, removed all diagnoses not assigned to it from the training data. We calculated average AUC only for events that were missing at each hospital. The high AUC means that compensation for missing events from other hospitals works well.

In the case of three hospitals as an example, we divided the most common 80 diagnoses into three groups of 27, 27, and 26 diagnoses and assigned each group to each hospital. The first hospital can have only 27 diagnoses assigned to it, and the other 53 diagnoses were removed, i.e., none of the patients in the first hospital had any of these 53 diagnoses. As a result, the local embedding model in the first hospital does not have the embeddings of removed diagnoses. However, embeddings for missing diagnoses are necessary to make predictions and measure prediction accuracy for them. In an ideal situation that all hospitals can share raw EHR to construct the global embedding model, the average AUC for these 53 diagnoses can be easily computed (Fig. 5a, "Global" Site 1). Without the global embedding model, if no other information is available, the first hospital could represent the embeddings of missing events naïvely by using random vectors to compute the average AUC (Fig. 5a, "Random" Site 1). Instead of random vectors, local embeddings from other hospitals could substitute for them (Fig. 5a, "Local" Site 1). Likewise, harmonized embeddings can compensate for missing diagnoses to compute the average AUC (Fig. 5a, "ProT" and "EncT" Site 1). The other two hospitals were treated in the same way.

Experimental results were obtained for the cases of three to five hospitals (Fig. 5). When the embeddings of missing events were represented naïvely using random vectors, the AUC was indistinguishable from the random prediction (AUC = 0.5). Furthermore, importing the local embeddings of another hospital did not significantly improve the average AUC because the embeddings lie in different spaces. However, the use of embeddings of other hospitals after harmonization yielded a significant increase in AUC. HarmoAE achieved a higher mean AUC than Procrustes at all numbers of hospitals; the difference was significant (paired t-test; $p < 0.01$) except for the 10% corresponding pairs.

3.3.2. Split patient history

In reality, each patient visits several hospitals. No hospital can access the patients' clinical pathways from other hospitals, so each hospital can use only part of the clinical pathway to predict future diagnoses. This limitation makes predictions somewhat inaccurate even with the harmonized embedding model. To make an accurate prediction, hospitals first calculate local patient vectors using the partial clinical pathways, sum these locally-calculated patient vectors, and normalize the summed vectors. These vectors approximate global patient vectors. In this procedure, hospitals share only local patient vectors that already compressed a sufficient number of medical event vectors, so this sharing does not disclose sensitive records of patients. With approximated global patient vectors, each hospital can consider the overall clinical pathways of patients, so improve prediction accuracy.

To explain the experiment in detail, suppose that patients can visit three hospitals. We simulated the situation by dividing the records of patients into three parts and randomly assigning them to one of the hospitals; as a result, each hospital had one-third of records for each patient. In cases that harmonized embeddings were not available, each hospital used these partial records to compute local patient vectors and made predictions using these patient vectors and local embeddings (Fig. 6a, "Local" Partial). Alternatively, to exploit scattered clinical pathways, hospitals summed and normalized patient vectors in them to compute approximated global patient vectors (Fig. 6a, "Local" Comb.). With the harmonized embeddings, each hospital also computed patient vectors using only partial records and made predictions (Fig. 6a, "ProT" and "EncT" Partial). As above, with the harmonized embeddings, hospitals computed approximated global patient vectors by utilizing patient vectors calculated in the three hospitals together (Fig. 6a, "ProT" and "EncT" Comb.).

Experimental results were obtained for cases that the patients visit three, four, or five hospitals (Fig. 6). When scattered records were not fully exploited, predictions provided poor accuracy regardless of whether embeddings were harmonized or not. When we used local embeddings that lie in different spaces, the method that combines patient vectors in three hospitals showed somewhat increased AUC, but it was still much lower than ideal AUC "Global". After harmonization, regardless of "ProT" and "EncT", the use of combined patient vectors achieved higher AUC than the use of local patient vectors. In particular, "EncT" showed significantly higher AUC than "ProT". The average AUC decreased as the number of hospitals increased, because the dataset was finely divided so the amount of training data for learning local embeddings was reduced at each hospital. "EncT" was significantly more accurate (paired t-test; $p < 0.01$) than "ProT" when combined patient vectors were used, but not when local vectors were used.

3.3.3. Hospitals with different sizes

A small or new hospital may collect biased data. The bias can lead to incorrect or uninformative local embeddings, which causes a decrease in the prediction accuracy. Harmonization with embeddings in a large hospital can alleviate the problem. To simulate the situation, we divided data in the training set into one large hospital and several small hospitals. Each small hospital had 5% and 10% of the total training data; the large hospital had the rest.

Experimental results were obtained for three, four, or five hospitals, with split ratios for each. For each case, we calculated the average AUC of hospitals that correspond to the proportions below the graph (Fig. 7). Overall, due to insufficient data, the

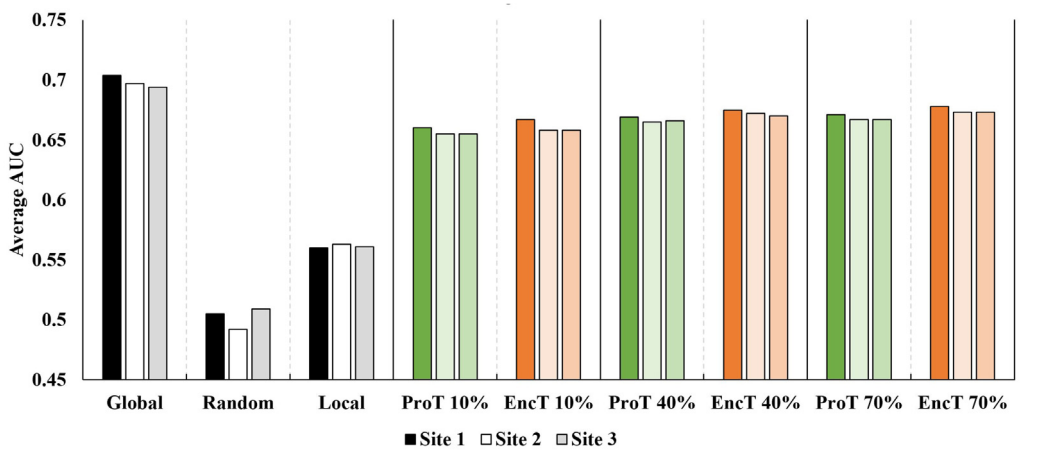

(a) 3 hospitals.

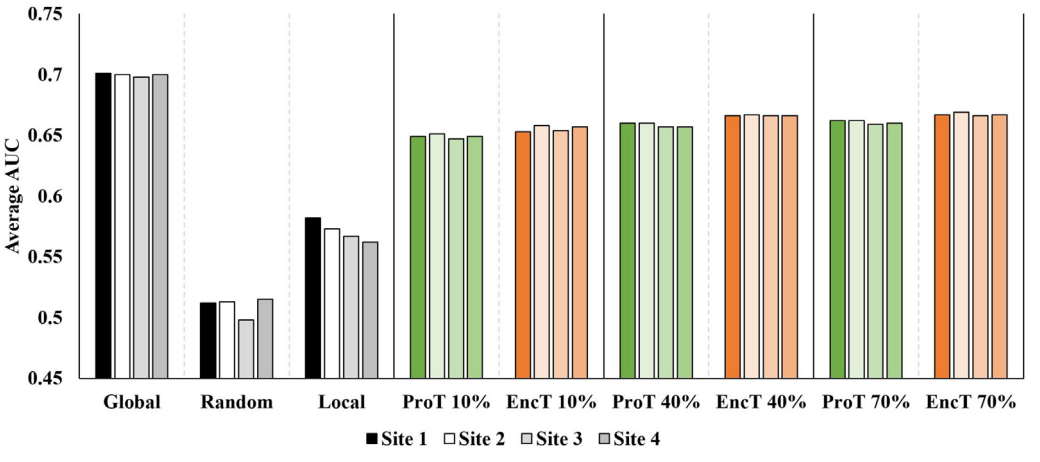

(b) 4 hospitals.

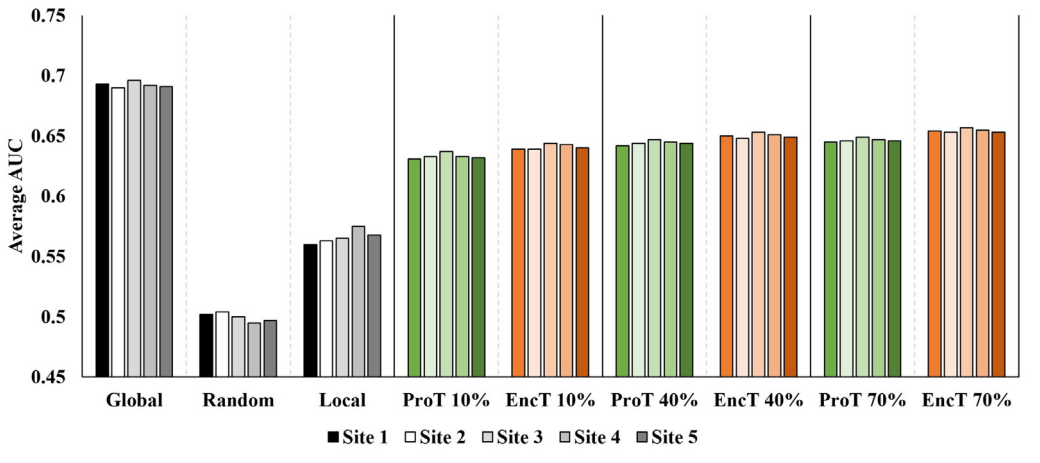

(c) 5 hospitals.

Fig. 5. Average AUC in the scenario "Incomplete information". "Global" is the average AUC using the global embedding model, which is an ideal accuracy of our predictive modeling. The legend applies the same way to the rest.

small hospitals showed significantly lower AUC than the large hospital. Regardless of the ratio of the corresponding pairs, the results were the same as below. "ProT" did not produce a noticeable AUC improvement in small hospitals even over "Local", whereas "EncT" noticeably increased the AUC in small hospitals by harmonizing embeddings of small hospitals with the

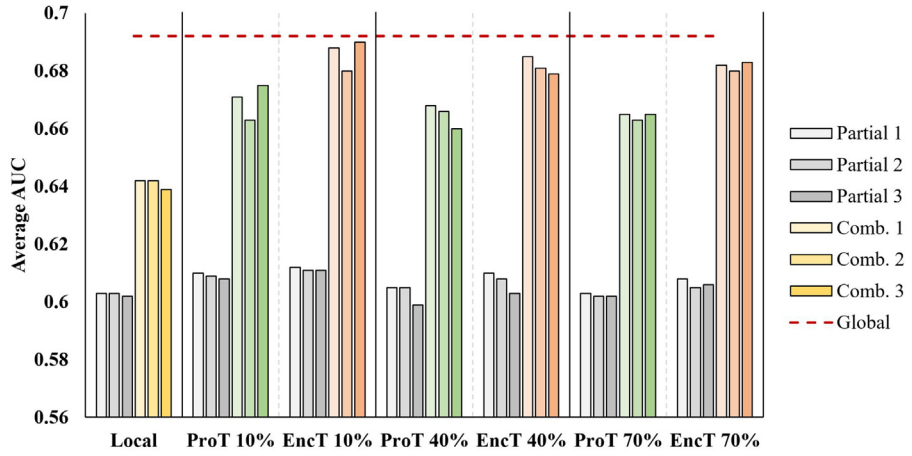

(a) 3 hospitals.

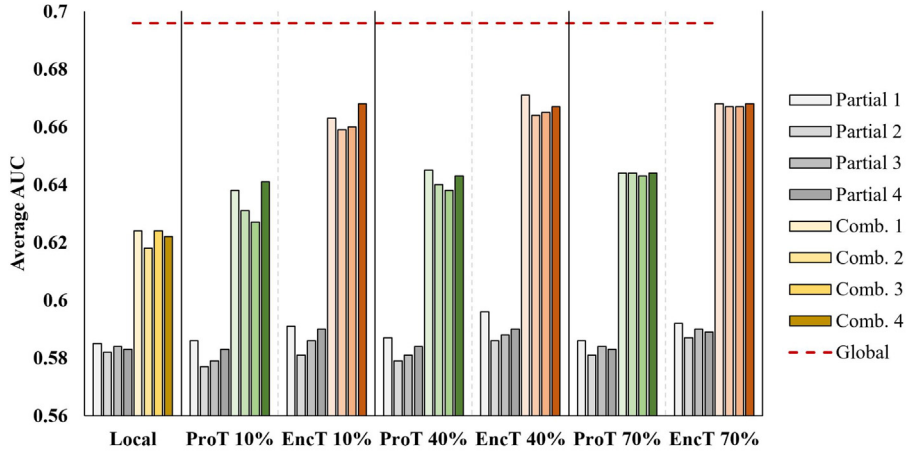

(b) 4 hospitals.

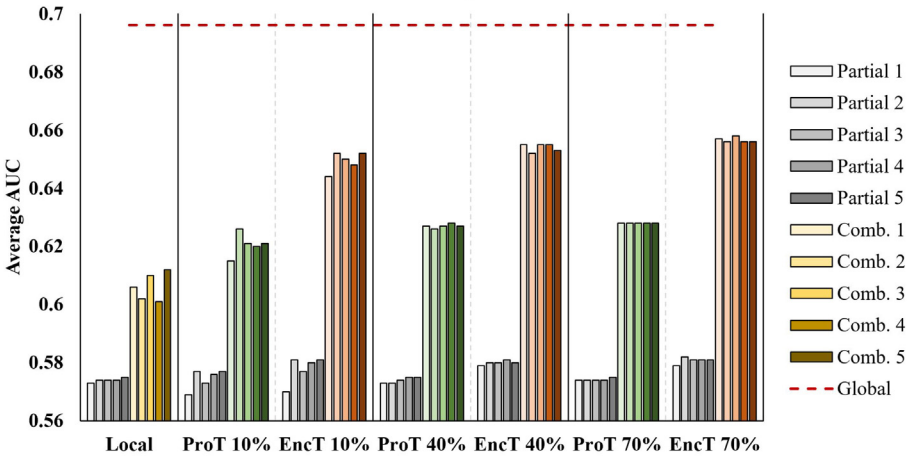

(c) 5 hospitals.

Fig. 6. Average AUC in the scenario "Split patient history". "Partial": average AUC using patient vectors derived from partial clinical pathways of the hospital. "Combined": average AUC using approximated global patient vectors. The legend applies the same way to the rest.

embeddings of large hospitals. However, the AUC of the large hospital decreased after embeddings were harmonized using HarmoAE. The decrease may occur because the proposed method adjusts not only embeddings in small hospitals but also the embeddings in large hospitals to harmonize these embeddings.

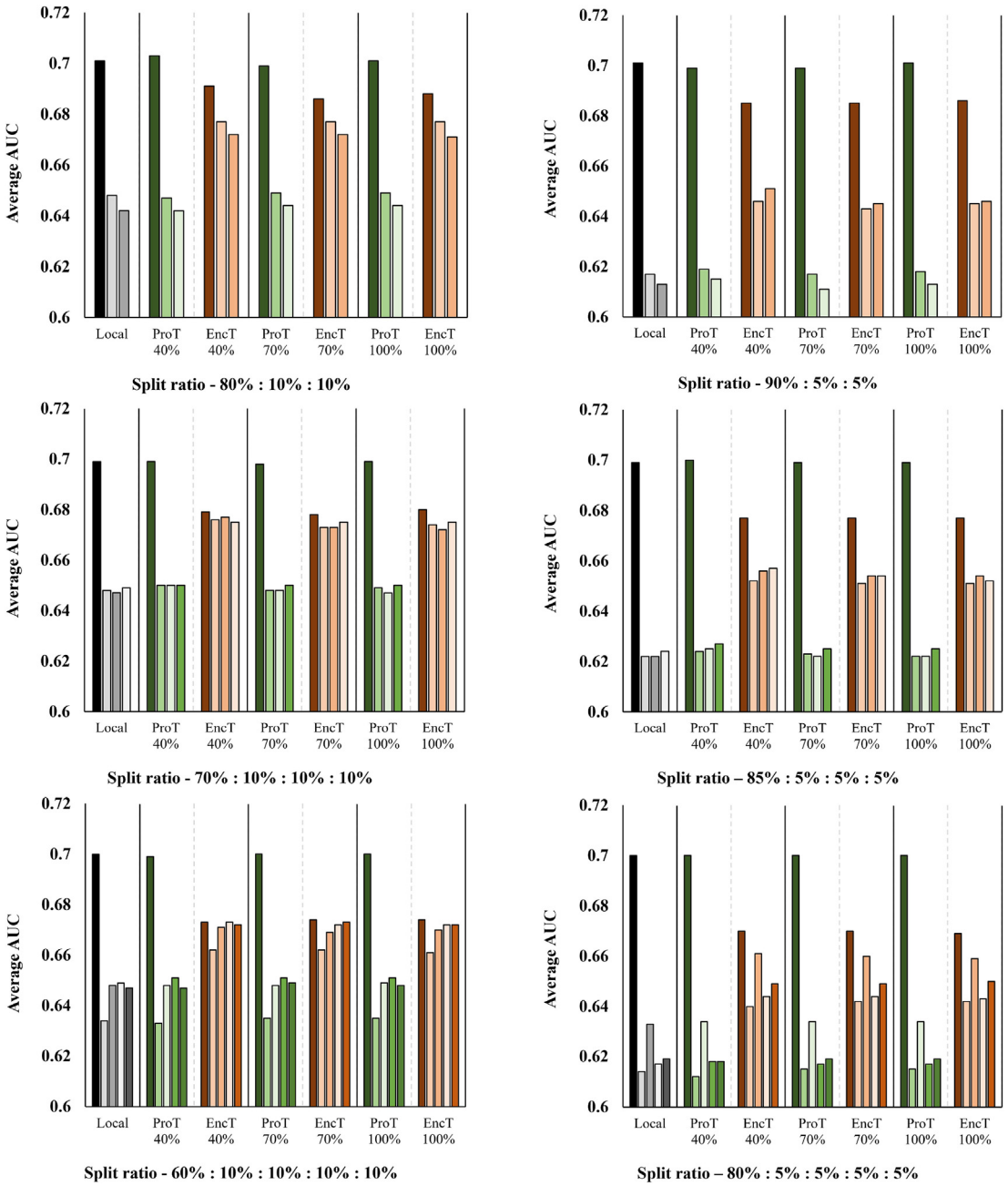

Fig. 7. Average AUC in the scenario "Hospitals with different sizes" when HarmoAE is trained without two-phase training. Results for 3 hospitals (top row), 4 hospitals (middle row), and 5 hospitals (bottom row). Split ratio: percentages of data in a large hospital and remaining hospitals. The first bar in each part of graphs corresponds to the large hospital, and remaining bars to small hospitals.

We applied two-phase training to prevent the distortion of contextual information during the harmonization (Fig. 8). A notable difference from Fig. 7 is that the average AUC in the large hospital did not show any performance degradation. This result means that the two-phase training successfully maintained the contextual information in embeddings of the large hospital. Additionally, with HarmoAE, by exploiting maintained contextual information in the large hospital, the small hospitals showed a slightly increased average AUC compared to the AUC without two-phase training. The AUC of the large hospital was highest in "EncT" by discovering useful low-dimensional manifolds. "EncT" achieved significantly higher AUC than "ProT" (paired t-test; $p < 0.01$) in all cases regardless of the size of hospitals.

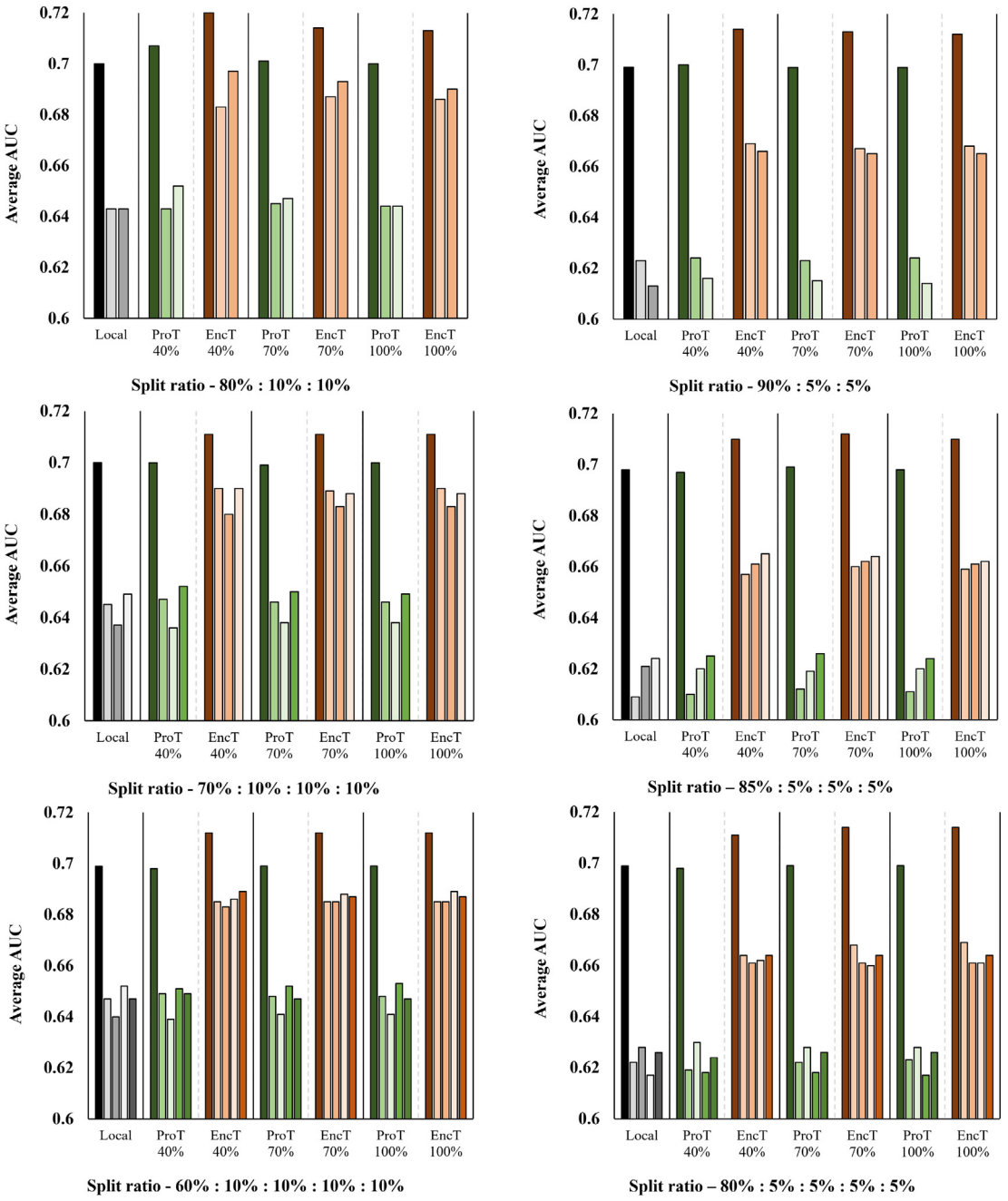

Fig. 8. Average AUC in the scenario "Hospitals with different sizes" when HarmoAE is trained with the two-phase training. Experimental results for 3 hospitals (top row), 4 hospitals (middle row), and 5 hospitals (bottom row).

4. Discussion

For privacy-preserving predictive analysis, this study proposes HarmoAE to harmonize contextual embeddings in different spaces. HarmoAE can efficiently and simultaneously harmonize the embeddings of multiple hospitals in one model, whereas the previous work uses Procrustes that projects embeddings in one space directly into the other space for only two spaces at a time, so harmonization is implemented independently for all pairs of hospitals. Also, during the harmonization procedure, HarmoAE learns a non-linear mapping from local embeddings into the harmonized embeddings, and discovers low-dimensional manifolds by considering corresponding information between all pairs of hospitals. With this efficient

harmonization, HarmoAE significantly improved the prediction accuracy in diverse situations. In a few worst cases, it achieved only similar accuracy to the existing method.

HarmoAE can be extended easily to include new hospitals by using corresponding pairs with any hospital. Therefore, HarmoAE can easily harmonize more information and lead to more accurate prediction compared to the existing method. In contrast, to integrate embeddings of new hospitals, the existing method requires that each new hospital have enough corresponding pairs with the base hospital; otherwise, embeddings must be transformed sequentially through spaces of other hospitals with corresponding pairs, and this process may cause information loss in embeddings.

This study has some limitations. We randomly divided a single dataset, MIMIC-III, and simulated the distributed environment in a single machine. Randomly-divided parts that represent different hospitals originate from the same dataset, so they can be harmonized more successfully than reality, and this result may artificially boost the prediction accuracy. Heterogeneous datasets are difficult to harmonize using simple models, so the use of encoders and decoders that have only one layer might not work successfully. Therefore, the use of encoders and decoders with more than one layer need to be tested for them. Furthermore, although HarmoAE is readily applicable to the case of many hospitals, the experimental results of the scenario "Incomplete information" with nine hospitals (Appendix B) show no significant improvement. A single dataset was finely partitioned, so contextual embeddings from each hospital deteriorated as the number of patients in each hospital decreased, and as a result, the prediction accuracy decreased. This deterioration might reduce the difference in prediction accuracy between HarmoAE and the previous method. Meanwhile, in addition to predictive accuracy, further analyses should simulate diverse environments of organizations that have different computing resources.

The same medical events could have different semantics or even conflict with each other in some hospitals, and this problem was not considered in this study. Some of these events might be used as corresponding pairs; if so, placing their embeddings close in the space of harmonized embeddings may lead to wrong harmonized embeddings. This heterogeneity would be further studied in future work. We may hold both embeddings of the same event with different semantics, whereas we could unify embeddings that have the same semantics to improve the prediction accuracy.

Immediate future work is to find the best implementation for each component of the privacy-preserving predictive framework used in this study (Fig. 1). To isolate the performance difference due to the change of the harmonization method, the framework remained the same as the previous work [17] except for the harmonization part. However, the use of cutting-edge methods regarding each of the components might improve the results. For example, many recent embedding models aforementioned and some studies of bilingual autoencoders [3,44] can be the alternatives in the first and second step, respectively. Comparison of the efficiency and accuracy further achieved using these substitutions might yield insights.

Another future research direction is to integrate the whole predictive framework in an end-to-end learning context. In this study, we trained each component of the framework independently. For example, learning contextual embeddings in each hospital or training HarmoAE does not consider the predictive analysis after that. The learning and harmonization of embedding, calculation of patient vectors, and future diagnostic predictions could be continuously stacked in a single model to build an optimal model for a final predictive task rather than for separate processes. Instead of sequentially stacking tasks, some recent studies trained models jointly by using a combined cost function that consists of costs for different tasks and achieved good performance [18,9]. This success implies that we could also build a model that harmonizes embeddings while simultaneously minimizing prediction errors.

Reducing the model complexity could be a remaining task. In this study, we trained independent mapping for each hospital to handle separate spaces of embeddings. However, although embeddings in different hospitals lie in separate spaces, some hospitals have similar contextual information in EHRs; as a result, there may exist geometric properties that we can exploit to harmonize embeddings. In further research, we would try to find and use these geometric commonalities to lessen the model complexity required for efficient harmonization. We can also reduce computation and time complexity by using only a fraction of corresponding pairs at each iteration. Some studies of language and data embedding have shown that stochastic sampling can decrease the complexity while retaining model performance [2,19]. Lastly, to achieve maximum efficiency, we would find the minimum number of corresponding pairs that can maintain the harmonization performance.

5. Conclusion

Contextual embedding has been successfully used for predictive tasks. A contextual embedding does not contain patient-level data, so it is relatively free from the risk of revealing private information. Due to this, unlike other privacy-preserving methods, sharing embeddings does not require rigorous and expensive privacy and security techniques such as DP, HE, or MPC. However, to use the embeddings independently learned in each hospital together, they must be aligned in one space. To this end, this paper proposed a novel method that extends a bilingual autoencoder to achieve efficient harmonization of embeddings that are learned from numerous hospitals. The proposed method utilizes the corresponding information between all pairs of hospitals in the model, learns non-linear transformation, and finds useful representations. As a result, the proposed method showed significantly improved alignment and prediction accuracy over the existing method in most experiments with multiple hospitals. Also, in an experimental scenario that considered hospitals of different sizes, the proposed two-phase training method increased the prediction accuracies for both large and small hospitals. This result may motivate large hospitals to participate in the model, and the involvement of large hospitals is crucial because it dominates the overall predictive performance. Several complications remain to be further studied, such as heterogeneity of data, differ-

ent computing resources between sources, and model complexity, but nevertheless, the proposed method allows the construction of a harmonized contextual embedding model with no assumption that data are distributed horizontally or vertically, so it can be a useful and practical alternative to existing distributed models for predictive tasks.

CRediT authorship contribution statement

Taek-Ho Lee: Methodology, Software, Writing - original draft. **Junghye Lee:** Conceptualization, Methodology, Supervision, Writing - review & editing. **Chi-Hyuck Jun:** Supervision, Writing - review & editing.

Declaration of Competing Interest

The authors declare that they have no known competing financial interests or personal relationships that could have appeared to influence the work reported in this paper.

Acknowledgements

This work was supported by the National Research Foundation of Korea (NRF) grant funded by the Korea government (MEST) (No. 2020R1A2C1005442 and No. 2020R1C1C1011063); The work was also supported by Institute of Information & communications Technology Planning & Evaluation (IITP) grant funded by the Korea government (MSIT) (No.2020-0-01336, Artificial Intelligence graduate school support (UNIST)).

Appendix A. Experimental results of "Alignment

See Table A.1–A.4.

Table A.1
Average PCN (standard deviation) over 10 repetitions in the case of three hospitals. Bold: the significantly higher average PCN in the paired t-test.

Alignment	*K*			
	1	10	50	100
Original	0.001 (0.000)	0.0078 (0.001)	0.0319 (0.002)	0.0603 (0.001)
ProT 40%	0.1654 (0.002)	0.3536 (0.004)	0.5346 (0.004)	0.629 (0.003)
EncT 40%	**0.2268**** **(0.004)**	**0.4262**** **(0.005)**	**0.5758**** **(0.006)**	**0.6528**** **(0.005)**
Original	0.001 (0.000)	0.0081 (0.001)	0.0339 (0.002)	0.0619 (0.002)
ProT 70%	0.2164 (0.003)	0.4097 (0.004)	0.5766 (0.006)	0.6634 (0.005)
EncT 70%	**0.2643**** **(0.003)**	**0.4713**** **(0.004)**	**0.6131**** **(0.005)**	**0.6867**** **(0.005)**
Original	0.0009 (0.000)	0.0076 (0.002)	0.0317 (0.003)	0.0592 (0.003)
ProT 100%	0.2502 (0.003)	0.4389 (0.003)	0.5973 (0.003)	0.6797 (0.003)
EncT 100%	**0.2775**** **(0.003)**	**0.4865**** **(0.004)**	**0.6263**** **(0.005)**	**0.6985**** **(0.004)**

$^{**}p < .01$.

Table A.2
Average PCN (standard deviation) over 10 repetitions in the case of four hospitals. Bold: the significantly higher average PCN in the paired t-test.

Alignment	*K*			
	1	10	50	100
Original	0.0011 (0.000)	0.0088 (0.001)	0.0355 (0.002)	0.0656 (0.003)
ProT 40%	0.1348 (0.003)	0.3155 (0.006)	0.5052 (0.007)	0.6076 (0.006)
EncT 40%	**0.2013**** **(0.003)**	**0.403**** **(0.007)**	**0.5627**** **(0.006)**	**0.6461**** **(0.007)**
Original	0.001 (0.000)	0.0086 (0.001)	0.0353 (0.003)	0.0651 (0.003)
ProT 70%	0.1823 (0.003)	0.3732 (0.005)	0.5513 (0.005)	0.6444 (0.005)
EncT 70%	**0.2355**** **(0.003)**	**0.4442**** **(0.003)**	**0.5956**** **(0.004)**	**0.6753**** **(0.005)**
Original	0.001 (0.000)	0.0086 (0.001)	0.0353 (0.003)	0.0647 (0.004)
ProT 100%	0.215 (0.002)	0.4007 (0.003)	0.5681 (0.003)	0.6566 (0.003)
EncT 100%	**0.2471**** **(0.003)**	**0.4544**** **(0.003)**	**0.605**** **(0.003)**	**0.6826**** **(0.003)**

$^{**}p < .01$.

Table A.3
Average PCN (standard deviation) over 10 repetitions in the case of five hospitals. Bold: the significantly higher average PCN in the paired t-test.

Alignment	*K*			
	1	10	50	100
Original	0.001 (0.000)	0.01 (0.001)	0.0395 (0.001)	0.0727 (0.002)
ProT 40%	0.1201 (0.003)	0.2989 (0.004)	0.4898 (0.004)	0.5947 (0.004)
EncT 40%	**0.1881**** **(0.003)**	**0.3901**** **(0.003)**	**0.5521**** **(0.003)**	**0.6383**** **(0.003)**
Original	0.0011 (0.000)	0.0094 (0.001)	0.0384 (0.002)	0.0702 (0.002)
ProT 70%	0.1621 (0.002)	0.3476 (0.005)	0.5288 (0.006)	0.6259 (0.005)
EncT 70%	**0.2132**** **(0.002)**	**0.4179**** **(0.005)**	**0.5761**** **(0.005)**	**0.6592**** **(0.004)**
Original	0.001 (0.000)	0.009 (0.001)	0.0383 (0.002)	0.0708 (0.003)
ProT 100%	0.1924 (0.002)	0.3767 (0.004)	0.5484 (0.004)	0.6399 (0.004)
EncT 100%	**0.2227**** **(0.002)**	**0.4294**** **(0.004)**	**0.5854**** **(0.004)**	**0.6679**** **(0.004)**

$^{**}p < .01$.

Table A.4
Average PCN (standard deviation) over 10 repetitions in the case of nine hospitals. Bold: the significantly higher average PCN in the paired t-test.

Alignment	*K*			
	1	10	50	100
Original	0.001 (0.000)	0.0113 (0.000)	0.0462 (0.002)	0.0853 (0.003)
ProT 40%	0.0966 (0.002)	0.267 (0.004)	0.4594 (0.004)	0.5658 (0.004)
EncT 40%	**0.1502 (0.002)**	**0.348 (0.003)**	**0.5204 (0.003)**	**0.6139 (0.003)**
Original	0.0013 (0.000)	0.0113 (0.001)	0.0468 (0.002)	0.0862 (0.002)
ProT 70%	0.1261 (0.001)	0.2995 (0.003)	0.4826 (0.003)	0.5843 (0.003)
EncT 70%	**0.1613 (0.002)**	**0.3596 (0.003)**	**0.5293 (0.003)**	**0.6214 (0.003)**
Original	0.0011 (0.000)	0.0111 (0.001)	0.0464 (0.002)	0.0852 (0.002)
ProT 100%	0.1486 (0.001)	0.3182 (0.003)	0.4943 (0.004)	0.5933 (0.004)
EncT 100%	**0.1661 (0.002)**	**0.364 (0.003)**	**0.5341 (0.004)**	**0.6261 (0.004)**

$^{**}p < .01$.

Appendix B. Experimental results of "Incomplete information

See Tables B.1–B.4.

Table B.1
Average AUC (standard deviation) over 10 repetitions of three hospitals. Bold: the significantly higher average AUC in the paired t-test.

Site	Global	Random	Local	ProT 10%	EncT 10%	ProT 40%	EncT 40%	ProT 70%	EncT 70%
1	0.704 (0.007)	0.505 (0.026)	0.56 (0.011)	0.66 (0.014)	**0.667*** **(0.013)**	0.669 (0.013)	**0.675**** (0.013)	0.671 (0.013)	**0.678**** (0.012)
2	0.697 (0.008)	0.492 (0.027)	0.563 (0.015)	0.655 (0.017)	0.658 (0.01)	0.665 (0.017)	**0.672**** **(0.018)**	0.667 (0.017)	**0.673**** **(0.016)**
3	0.694 (0.011)	0.509 (0.027)	0.561 (0.018)	0.655 (0.015)	0.658 (0.011)	0.666 (0.012)	**0.67**** **(0.011)**	0.667 (0.012)	**0.673**** **(0.01)**

$^{**}p < .01$. $^{*}p < .05$.

Table B.2
Average AUC (standard deviation) over 10 repetitions of four hospitals. Bold: the significantly higher average AUC in the paired t-test.

Site	Global	Random	Local	ProT 10%	EncT 10%	ProT 40%	EncT 40%	ProT 70%	EncT 70%
1	0.701 (0.009)	0.512 (0.027)	0.582 (0.014)	0.649 (0.009)	0.653 (0.009)	0.66 (0.006)	**0.666**** **(0.007)**	0.662 (0.006)	**0.667**** **(0.006)**
2	0.7 (0.007)	0.513 (0.028)	0.573 (0.013)	0.651 (0.01)	**0.658**** **(0.01)**	0.66 (0.009)	**0.667**** **(0.008)**	0.662 (0.01)	**0.669**** **(0.009)**
3	0.698 (0.009)	0.498 (0.025)	0.567 (0.019)	0.647 (0.007)	**0.654*** **(0.009)**	0.657 (0.007)	**0.666**** **(0.008)**	0.659 (0.008)	**0.666**** **(0.007)**
4	0.7 (0.008)	0.515 (0.028)	0.562 (0.021)	0.649 (0.008)	**0.657**** **(0.008)**	0.657 (0.007)	**0.666**** **(0.007)**	0.66 (0.007)	**0.667**** **(0.007)**

$^{**}p < .01$. $^{*}p < .05$.

Table B.3
Average AUC (standard deviation) over 10 repetitions of five hospitals. Bold: the significantly higher average AUC in the paired t-test.

Site	Global	Random	Local	ProT 10%	EncT 10%	ProT 40%	EncT 40%	ProT 70%	EncT 70%
1	0.693 (0.008)	0.502 (0.025)	0.56 (0.014)	0.631 (0.01)	**0.639**** **(0.007)**	0.642 (0.009)	**0.65**** **(0.006)**	0.645 (0.008)	**0.654**** **(0.008)**
2	0.69 (0.008)	0.504 (0.024)	0.563 (0.01)	0.633 (0.01)	0.639 (0.006)	0.644 (0.007)	**0.648**** **(0.006)**	0.646 (0.008)	**0.653**** **(0.007)**
3	0.696 (0.009)	0.5 (0.016)	0.565 (0.016)	0.637 (0.008)	**0.644*** **(0.008)**	0.647 (0.008)	**0.653*** **(0.006)**	0.649 (0.008)	**0.657**** **(0.006)**
4	0.692 (0.011)	0.495 (0.014)	0.575 (0.025)	0.633 (0.011)	**0.643**** **(0.01)**	0.645 (0.01)	**0.651*** **(0.008)**	0.647 (0.01)	**0.655**** **(0.009)**
5	0.691 (0.007)	0.497 (0.016)	0.568 (0.016)	0.632 (0.008)	**0.64*** **(0.009)**	0.644 (0.009)	**0.649**** **(0.006)**	0.646 (0.009)	**0.653**** **(0.005)**

$^{**}p < .01$. $^{*}p < .05$.

Table B.4
Average AUC (standard deviation) over 10 repetitions of nine hospitals. Bold: the significantly higher average AUC in the paired t-test.

Site	Global	Random	Local	ProT 10%	EncT 10%	ProT 40%	EncT 40%	ProT 70%	EncT 70%
1	0.69 (0.012)	0.496 (0.016)	0.561 (0.013)	0.621 (0.01)	**0.629*** **(0.014)**	0.631 (0.013)	0.634 (0.015)	0.633 (0.013)	0.634 (0.015)
2	0.688 (0.008)	0.493 (0.025)	0.564 (0.018)	0.622 (0.01)	**0.628*** **(0.008)**	0.633 (0.01)	0.632 (0.007)	0.633 (0.009)	0.633 (0.007)
3	0.689 (0.008)	0.486 (0.035)	0.571 (0.011)	0.621 (0.01)	0.626 (0.008)	0.631 (0.009)	0.63 (0.007)	0.633 (0.008)	0.631 (0.008)
4	0.688 (0.008)	0.489 (0.03)	0.562 (0.02)	0.621 (0.012)	**0.626*** **(0.011)**	0.63 (0.013)	0.63 (0.01)	0.632 (0.012)	0.631 (0.01)
5	0.691 (0.009)	0.499 (0.025)	0.57 (0.022)	0.623 (0.01)	**0.633**** **(0.007)**	0.635 (0.009)	0.634 (0.008)	0.636 (0.009)	0.635 (0.009)
6	0.688 (0.009)	0.491 (0.024)	0.565 (0.009)	0.622 (0.014)	**0.629*** **(0.007)**	0.633 (0.011)	0.632 (0.007)	0.633 (0.01)	0.633 (0.007)
7	0.689 (0.008)	0.509 (0.027)	0.565 (0.015)	0.621 (0.007)	**0.628**** **(0.007)**	0.631 (0.007)	0.632 (0.006)	0.634 (0.008)	0.633 (0.008)
8	0.689 (0.007)	0.498 (0.024)	0.568 (0.015)	0.622 (0.011)	0.627 (0.007)	0.631 (0.01)	0.63 (0.006)	0.633 (0.009)	0.631 (0.006)
9	0.689 (0.01)	0.503 (0.022)	0.569 (0.011)	0.621 (0.01)	**0.629*** **(0.009)**	0.631 (0.011)	0.632 (0.011)	0.633 (0.01)	0.633 (0.011)

$^{**}p < .01$. $^{*}p < .05$.

Appendix C. Experimental results of "Split patient history

See Tables C.1–C.4.

Table C.1
Average AUC (standard deviation) over 10 repetitions of three hospitals. Bold: the significantly higher average AUC in the paired t-test.

Site	Global	Original	ProT 10%	EncT 10%	ProT 40%	EncT 40%	ProT 70%	EncT 70%
Local 1	0.692 (0.009)	0.603 (0.011)	0.61 (0.023)	0.612 (0.025)	0.605 (0.012)	**0.61**** **(0.012)**	0.603 (0.01)	**0.608**** **(0.01)**
Local 2	0.692 (0.009)	0.603 (0.008)	0.609 (0.023)	0.611 (0.025)	0.605 (0.012)	**0.608*** **(0.013)**	0.602 (0.008)	**0.605*** **(0.008)**
Local 3	0.692 (0.009)	0.602 (0.008)	0.608 (0.015)	0.611 (0.014)	0.599 (0.007)	**0.603**** **(0.008)**	0.602 (0.009)	**0.606**** **(0.01)**
Combined 1	0.692 (0.009)	0.642 (0.013)	0.671 (0.028)	**0.688**** **(0.029)**	0.668 (0.011)	**0.685**** **(0.011)**	0.665 (0.008)	**0.682**** **(0.009)**
Combined 2	0.692 (0.009)	0.642 (0.014)	0.663 (0.037)	**0.68**** **(0.035)**	0.666 (0.016)	**0.681**** **(0.016)**	0.663 (0.011)	**0.68**** **(0.01)**
Combined 3	0.692 (0.009)	0.639 (0.012)	0.675 (0.02)	**0.69**** **(0.018)**	0.66 (0.009)	**0.679**** **(0.006)**	0.665 (0.011)	**0.683**** **(0.009)**

$^{**}p < .01$. $^{*}p < .05$.

Table C.2
Average AUC (standard deviation) over 10 repetitions of four hospitals. Bold: the significantly higher average AUC in the paired t-test.

Site	Global	Original	ProT 10%	EncT 10%	ProT 40%	EncT 40%	ProT 70%	EncT 70%
Local 1	0.696 (0.005)	0.585 (0.009)	0.586 (0.016)	0.591 (0.017)	0.587 (0.01)	**0.596**** **(0.01)**	0.586 (0.009)	**0.592**** **(0.01)**
Local 2	0.696 (0.005)	0.582 (0.005)	0.577 (0.017)	**0.581*** **(0.019)**	0.579 (0.007)	**0.586**** **(0.007)**	0.581 (0.005)	**0.587**** **(0.006)**
Local 3	0.696 (0.005)	0.584 (0.008)	0.579 (0.013)	**0.586**** **(0.015)**	0.581 (0.009)	**0.588**** **(0.01)**	0.584 (0.008)	**0.59**** **(0.01)**
Local 4	0.696 (0.005)	0.583 (0.009)	0.583 (0.013)	**0.59*** **(0.014)**	0.584 (0.01)	**0.59**** **(0.011)**	0.583 (0.01)	**0.589**** **(0.011)**
Combined 1	0.696 (0.005)	0.624 (0.01)	0.638 (0.025)	**0.663**** **(0.019)**	0.645 (0.011)	**0.671**** **(0.008)**	0.644 (0.009)	**0.668**** **(0.01)**
Combined 2	0.696 (0.005)	0.618 (0.012)	0.631 (0.022)	**0.659**** **(0.027)**	0.64 (0.009)	**0.664**** **(0.01)**	0.644 (0.007)	**0.667**** **(0.009)**
Combined 3	0.696 (0.005)	0.624 (0.008)	0.627 (0.021)	**0.66**** **(0.023)**	0.638 (0.011)	**0.665**** **(0.012)**	0.643 (0.007)	**0.667**** **(0.01)**
Combined 4	0.696 (0.005)	0.622 (0.011)	0.641 (0.019)	**0.668**** **(0.02)**	0.643 (0.006)	**0.667**** **(0.008)**	0.644 (0.005)	**0.668**** **(0.009)**

$^{**}p < .01$. $^{*}p < .05$.

Table C.3
Average AUC (standard deviation) over 10 repetitions of five hospitals. Bold: the significantly higher average AUC in the paired t-test.

Site	Global	Original	ProT 10%	EncT 10%	ProT 40%	EncT 40%	ProT 70%	EncT 70%
Local 1	0.696 (0.004)	0.573 (0.009)	0.569 (0.012)	0.57 (0.012)	0.573 (0.01)	**0.579**** **(0.01)**	0.574 (0.009)	**0.579**** **(0.008)**
Local 2	0.696 (0.004)	0.574 (0.006)	0.577 (0.009)	**0.581*** **(0.011)**	0.573 (0.007)	**0.58**** **(0.009)**	0.574 (0.006)	**0.582**** **(0.007)**
Local 3	0.696 (0.004)	0.574 (0.006)	0.573 (0.01)	**0.577*** **(0.009)**	0.574 (0.006)	**0.58**** **(0.006)**	0.574 (0.006)	**0.581**** **(0.006)**
Local 4	0.696 (0.004)	0.574 (0.009)	0.576 (0.013)	0.58 (0.013)	0.575 (0.01)	**0.581**** **(0.01)**	0.574 (0.009)	**0.581**** **(0.01)**
Local 5	0.696 (0.004)	0.575 (0.007)	0.577 (0.013)	**0.581**** **(0.013)**	0.575 (0.007)	**0.58**** **(0.008)**	0.575 (0.007)	**0.581**** **(0.006)**
Combined 1	0.696 (0.004)	0.606 (0.014)	0.615 (0.016)	**0.644**** **(0.017)**	0.627 (0.008)	**0.655** **(0.01)**	0.628 (0.005)	**0.657** **(0.007)**
Combined 2	0.696 (0.004)	0.602 (0.008)	0.626 (0.012)	**0.652** **(0.011)**	0.626 (0.006)	**0.652** **(0.008)**	0.628 (0.005)	**0.656** **(0.006)**
Combined 3	0.696 (0.004)	0.61 (0.018)	0.621 (0.013)	**0.65** **(0.014)**	0.627 (0.006)	**0.655** **(0.004)**	0.628 (0.004)	**0.658**** **(0.004)**
Combined 4	0.696 (0.004)	0.601 (0.012)	0.62 (0.014)	**0.648**** **(0.013)**	0.628 (0.008)	**0.655**** **(0.009)**	0.628 (0.006)	**0.656**** **(0.007)**
Combined 5	0.696 (0.004)	0.612 (0.008)	0.621 (0.015)	**0.652**** **(0.017)**	0.627 (0.004)	**0.653**** **(0.006)**	0.628 (0.004)	**0.656**** **(0.005)**

$^{**}p < .01$. $^{*}p < .05$.

Table C.4
Average AUC (standard deviation) over 10 repetitions of nine hospitals. Bold: the significantly higher average AUC in the paired t-test.

Site	Global	Original	ProT 10%	EncT 10%	ProT 40%	EncT 40%	ProT 70%	EncT 70%
Local 1	0.693 (0.005)	0.57 (0.011)	0.566 (0.011)	0.563 (0.01)	0.569 (0.01)	0.565 (0.009)	**0.57*** **(0.01)**	0.565 (0.009)
Local 2	0.693 (0.005)	0.574 (0.01)	0.573 (0.012)	0.57 (0.013)	0.574 (0.01)	0.572 (0.01)	0.574 (0.01)	0.571 (0.01)
Local 3	0.693 (0.005)	0.579 (0.008)	**0.576*** **(0.011)**	0.569 (0.011)	**0.579*** **(0.008)**	0.574 (0.007)	**0.579**** **(0.008)**	0.572 (0.006)
Local 4	0.693 (0.005)	0.569 (0.008)	0.564 (0.009)	0.56 (0.005)	**0.568*** **(0.008)**	0.565 (0.007)	0.568 (0.007)	0.566 (0.007)
Local 5	0.693 (0.005)	0.582 (0.007)	**0.581**** **(0.009)**	0.575 (0.011)	**0.582**** **(0.007)**	0.577 (0.008)	**0.582**** **(0.007)**	0.577 (0.007)
Local 6	0.693 (0.005)	0.575 (0.009)	0.571 (0.011)	0.567 (0.009)	**0.575*** **(0.009)**	0.571 (0.007)	0.575 (0.009)	0.572 (0.007)
Local 7	0.693 (0.005)	0.571 (0.006)	0.567 (0.01)	0.567 (0.013)	0.571 (0.006)	0.57 (0.007)	0.571 (0.006)	0.569 (0.007)
Local 8	0.693 (0.005)	0.576 (0.006)	**0.568**** **(0.011)**	0.564 (0.009)	**0.576*** **(0.006)**	0.573 (0.006)	**0.576**** **(0.006)**	0.572 (0.006)
Local 9	0.693 (0.005)	0.574 (0.008)	**0.573*** **(0.013)**	0.568 (0.013)	**0.574**** **(0.008)**	0.568 (0.005)	**0.574**** **(0.008)**	0.568 (0.007)
Combined 1	0.693 (0.005)	0.599 (0.018)	0.605 (0.011)	**0.63**** **(0.011)**	0.618 (0.008)	**0.634**** **(0.005)**	0.619 (0.007)	**0.634**** **(0.004)**
Combined 2	0.693 (0.005)	0.588 (0.02)	0.605 (0.012)	**0.631**** **(0.009)**	0.617 (0.008)	**0.636**** **(0.005)**	0.618 (0.007)	**0.636**** **(0.005)**
Combined 3	0.693 (0.005)	0.592 (0.016)	0.603 (0.01)	**0.629**** **(0.013)**	0.618 (0.007)	**0.637**** **(0.005)**	0.62 (0.007)	**0.637**** **(0.006)**
Combined 4	0.693 (0.005)	0.588 (0.017)	0.602 (0.008)	**0.625**** **(0.009)**	0.616 (0.007)	**0.633**** **(0.005)**	0.618 (0.006)	**0.634**** **(0.004)**
Combined 5	0.693 (0.005)	0.592 (0.015)	0.605 (0.011)	**0.629**** **(0.009)**	0.618 (0.007)	**0.636**** **(0.005)**	0.621 (0.006)	**0.637**** **(0.006)**
Combined 6	0.693 (0.005)	0.595 (0.013)	0.61 (0.009)	**0.632**** **(0.009)**	0.621 (0.007)	**0.639**** **(0.004)**	0.622 (0.008)	**0.638**** **(0.006)**
Combined 7	0.693 (0.005)	0.59 (0.011)	0.608 (0.012)	**0.634**** **(0.011)**	0.615 (0.006)	**0.635**** **(0.004)**	0.617 (0.006)	**0.635**** **(0.007)**
Combined 8	0.693 (0.005)	0.602 (0.01)	0.607 (0.014)	**0.63**** **(0.013)**	0.619 (0.006)	**0.638**** **(0.005)**	0.62 (0.006)	**0.638**** **(0.006)**
Combined 9	0.693 (0.005)	0.598 (0.016)	0.611 (0.013)	**0.635**** **(0.012)**	0.619 (0.011)	**0.636**** **(0.007)**	0.62 (0.011)	**0.636**** **(0.009)**

$^{**}p < .01$. $^{*}p < .05$.

Appendix D. Experimental results of "Hospitals with different sizes

See Tables D.1–D.4.

Table D.1
Average AUC (standard deviation) over 10 repetitions of three hospitals. Bold: the significantly higher average AUC in the paired t-test.

Ratio (size)	Original	ProT 40%	EncT 40%	ProT 70%	EncT 70%	ProT 100%	EncT 100%
80	0.7 (0.002)	0.707 (0.007)	**0.72**** **(0.008)**	0.701 (0.002)	**0.714**** **(0.004)**	0.7 (0.002)	**0.713**** **(0.003)**
10	0.643 (0.01)	0.643 (0.008)	**0.683**** **(0.009)**	0.645 (0.01)	**0.687**** **(0.008)**	0.644 (0.01)	**0.686**** **(0.009)**
10	0.643 (0.01)	0.652 (0.01)	**0.697**** **(0.008)**	0.647 (0.01)	**0.693**** **(0.008)**	0.644 (0.01)	**0.69**** **(0.006)**
90	0.699 (0.002)	0.7 (0.006)	**0.714**** **(0.009)**	0.699 (0.004)	**0.713**** **(0.005)**	0.699 (0.002)	**0.712**** **(0.003)**
5	0.623 (0.012)	0.624 (0.012)	**0.669**** **(0.015)**	0.623 (0.013)	**0.667**** **(0.013)**	0.624 (0.013)	**0.668**** **(0.01)**
5	0.613 (0.011)	0.616 (0.02)	**0.666**** **(0.022)**	0.615 (0.011)	**0.665**** **(0.012)**	0.614 (0.012)	**0.665**** **(0.011)**

$^{**}p < .01$. $^{*}p < .05$.

Table D.2
Average AUC (standard deviation) over 10 repetitions of four hospitals. Bold: the significantly higher average AUC in the paired t-test.

Ratio (size)	Original	ProT 40%	EncT 40%	ProT 70%	EncT 70%	ProT 100%	EncT 100%
70	0.7 (0.003)	0.7 (0.007)	**0.711**** **(0.008)**	0.699 (0.005)	**0.711**** **(0.006)**	0.7 (0.003)	**0.711**** **(0.003)**
10	0.645 (0.01)	0.647 (0.011)	**0.69**** **(0.011)**	0.646 (0.01)	**0.689**** **(0.008)**	0.646 (0.01)	**0.69**** **(0.009)**
10	0.637 (0.012)	0.636 (0.013)	**0.68**** **(0.011)**	0.638 (0.012)	**0.683**** **(0.009)**	0.638 (0.012)	**0.683**** **(0.01)**
10	0.649 (0.009)	0.652 (0.01)	**0.69**** **(0.01)**	0.65 (0.009)	**0.688**** **(0.006)**	0.649 (0.009)	**0.688**** **(0.006)**
85	0.698 (0.002)	0.697 (0.004)	**0.71**** **(0.005)**	0.699 (0.003)	**0.712**** **(0.004)**	0.698 (0.002)	**0.71**** **(0.003)**
5	0.609 (0.009)	0.61 (0.013)	**0.657**** **(0.011)**	0.612 (0.009)	**0.66**** **(0.008)**	0.611 (0.009)	**0.659**** **(0.007)**
5	0.621 (0.012)	0.62 (0.012)	**0.661**** **(0.013)**	0.619 (0.012)	**0.662**** **(0.013)**	0.62 (0.011)	**0.661**** **(0.011)**
5	0.624 (0.012)	0.625 (0.012)	**0.665**** **(0.014)**	0.626 (0.012)	**0.664**** **(0.01)**	0.624 (0.011)	**0.662**** **(0.009)**

$^{**}p < .01$. $^{*}p < .05$.

Table D.3
Average AUC (standard deviation) over 10 repetitions of five hospitals. Bold: the significantly higher average AUC in the paired t-test.

Ratio (size)	Original	ProT 40%	EncT 40%	ProT 70%	EncT 70%	ProT 100%	EncT 100%
60	0.699 (0.003)	0.698 (0.005)	**0.712**** **(0.005)**	0.699 (0.003)	**0.712**** **(0.004)**	0.699 (0.003)	**0.712**** **(0.003)**
10	0.647 (0.01)	0.649 (0.012)	**0.685**** **(0.011)**	0.648 (0.01)	**0.685**** **(0.009)**	0.648 (0.011)	**0.685**** **(0.009)**
10	0.64 (0.011)	0.639 (0.012)	**0.683**** **(0.014)**	0.641 (0.011)	**0.685**** **(0.009)**	0.641 (0.011)	**0.685**** **(0.01)**
10	0.652 (0.01)	0.651 (0.011)	**0.686**** **(0.01)**	0.652 (0.01)	**0.688**** **(0.01)**	0.653 (0.01)	**0.689**** **(0.009)**
10	0.647 (0.006)	0.649 (0.007)	**0.689**** **(0.007)**	0.647 (0.006)	**0.687**** **(0.002)**	0.647 (0.006)	**0.687**** **(0.003)**
80	0.699 (0.002)	0.698 (0.004)	**0.711**** **(0.006)**	0.699 (0.002)	**0.714**** **(0.003)**	0.699 (0.002)	**0.714**** **(0.003)**
5	0.622 (0.016)	0.619 (0.017)	**0.664**** **(0.016)**	0.622 (0.016)	**0.668**** **(0.015)**	0.623 (0.016)	**0.669**** **(0.016)**
5	0.628 (0.015)	0.63 (0.017)	**0.661**** **(0.015)**	0.628 (0.015)	**0.661**** **(0.012)**	0.628 (0.015)	**0.661**** **(0.012)**
5	0.617 (0.012)	0.618 (0.012)	**0.662**** **(0.013)**	0.618 (0.012)	**0.66**** **(0.011)**	0.617 (0.012)	**0.661**** **(0.01)**
5	0.626 (0.014)	0.624 (0.015)	**0.664**** **(0.008)**	0.626 (0.014)	**0.664**** **(0.008)**	0.626 (0.014)	**0.664**** **(0.008)**

$^{**}p < .01$. $^{*}p < .05$.

Table D.4
Average AUC (standard deviation) over 10 repetitions of nine hospitals. Bold: the significantly higher average AUC in the paired t-test.

Ratio (size)	Original	ProT 40%	EncT 40%	ProT 70%	EncT 70%	ProT 100%	EncT 100%
20	0.673 (0.008)	0.673 (0.008)	**0.699**** **(0.006)**	0.673 (0.008)	**0.7**** **(0.006)**	0.673 (0.008)	**0.7**** **(0.006)**
10	0.651 (0.01)	0.652 (0.01)	**0.678**** **(0.007)**	0.652 (0.01)	**0.675**** **(0.007)**	0.652 (0.01)	**0.678**** **(0.005)**
10	0.646 (0.012)	0.646 (0.012)	**0.67**** **(0.011)**	0.647 (0.012)	**0.669**** **(0.009)**	0.647 (0.012)	**0.67**** **(0.01)**
10	0.652 (0.006)	0.654 (0.006)	**0.68**** **(0.006)**	0.653 (0.006)	**0.677**** **(0.006)**	0.653 (0.006)	**0.68**** **(0.005)**
10	0.647 (0.013)	0.648 (0.013)	**0.674**** **(0.012)**	0.648 (0.014)	**0.672**** **(0.011)**	0.648 (0.014)	**0.675**** **(0.01)**
10	0.638 (0.012)	0.639 (0.012)	**0.67**** **(0.009)**	0.639 (0.012)	**0.669**** **(0.01)**	0.639 (0.012)	**0.671**** **(0.009)**
10	0.649 (0.01)	0.649 (0.01)	**0.675**** **(0.008)**	0.649 (0.01)	**0.675**** **(0.01)**	0.649 (0.01)	**0.676**** **(0.01)**
10	0.647 (0.01)	0.647 (0.01)	**0.673**** **(0.01)**	0.648 (0.01)	**0.673**** **(0.009)**	0.648 (0.01)	**0.673**** **(0.01)**
10	0.645 (0.008)	0.644 (0.008)	**0.671**** **(0.01)**	0.646 (0.009)	**0.672**** **(0.011)**	0.646 (0.009)	**0.674**** **(0.011)**
60	0.698 (0.003)	0.698 (0.004)	**0.711**** **(0.004)**	0.698 (0.003)	**0.711**** **(0.004)**	0.698 (0.003)	**0.711**** **(0.004)**
5	0.617 (0.021)	0.616 (0.019)	**0.655**** **(0.015)**	0.616 (0.02)	**0.656**** **(0.017)**	0.616 (0.02)	**0.655**** **(0.015)**
5	0.615 (0.013)	0.616 (0.013)	**0.656**** **(0.011)**	0.616 (0.013)	**0.659**** **(0.012)**	0.616 (0.013)	**0.657**** **(0.011)**
5	0.628 (0.014)	0.627 (0.014)	**0.662**** **(0.014)**	0.627 (0.015)	**0.661**** **(0.013)**	0.627 (0.015)	**0.66**** **(0.015)**
5	0.622 (0.017)	0.621 (0.017)	**0.66**** **(0.013)**	0.621 (0.016)	**0.659**** **(0.009)**	0.621 (0.016)	**0.658**** **(0.013)**
5	0.621 (0.016)	0.622 (0.016)	**0.657**** **(0.015)**	0.622 (0.016)	**0.656**** **(0.015)**	0.622 (0.016)	**0.656**** **(0.015)**
5	0.621 (0.012)	0.622 (0.012)	**0.657**** **(0.01)**	0.62 (0.012)	**0.657**** **(0.01)**	0.62 (0.012)	**0.656**** **(0.01)**
5	0.62 (0.016)	0.62 (0.016)	**0.654**** **(0.015)**	0.62 (0.016)	**0.655**** **(0.016)**	0.62 (0.016)	**0.657**** **(0.015)**
5	0.615 (0.014)	0.615 (0.015)	**0.653**** **(0.012)**	0.615 (0.015)	**0.653**** **(0.01)**	0.615 (0.015)	**0.651**** **(0.012)**

$^{**}p < .01$. $^{*}p < .05$.

Appendix E. The 80 most common diagnoses

See Table E.1.

Table E.1
The 80 most common diagnoses.

ICD	Description
8	Intestinal Infections due to other organisms
38	Septicemia
41	Bacterial infection in conditions classified elsewhere and of unspecified site
70	Viral hepatitis
112	Candidiasis
197	Secondary malignant neoplasm of respiratory and digestive systems
198	Secondary malignant neoplasm of other specified sites
244	Acquired hypothyroidism
250	Diabetes mellitus
263	Other and unspecified protein-calorie malnutrition
272	Disorders of lipoid metabolism

(*continued on next page*)

Table E.1 (*continued*)

ICD	Description
274	Gout
275	Disorders of mineral metabolism
276	Disorders of fluid, electrolyte, and acid-base balance
278	Overweight, obesity and other hyperalimentation
280	Iron deficiency anemias
285	Other and unspecified anemias
286	Coagulation defects
287	Purpura and other hemorrhagic conditions
288	Diseases of white blood cells
293	Transient mental disorders due to conditions classified elsewhere
294	Persistent mental disorders due to conditions classified elsewhere
300	Anxiety, dissociative and somatoform disorders
303	Alcohol dependence syndrome
305	Nondependent abuse of drugs
311	Depressive disorder, not elsewhere classified
327	Organic sleep disorders
338	Pain
345	Epilepsy and recurrent seizures
348	Other conditions of brain
357	Inflammatory and toxic neuropathy
362	Other retinal disorders
401	Essential hypertension
403	Hypertensive chronic kidney disease
410	Acute myocardial infarction
412	Old myocardial infarction
414	Other forms of chronic ischemic heart disease
416	Chronic pulmonary heart disease
424	Other diseases of endocardium
425	Cardiomyopathy
427	Cardiac dysrhythmias
428	Heart failure
438	Late effects of cerebrovascular disease
440	Atherosclerosis
441	Aortic aneurysm and dissection
443	Other peripheral vascular disease
453	Other venous embolism and thrombosis
456	Varicose veins of other sites
458	Hypotension
482	Other bacterial pneumonia
486	Pneumonia, organism unspecified
491	Chronic bronchitis
493	Asthma
496	Chronic airway obstruction, not elsewhere classified
507	Pneumonitis due to solids and liquids
511	Pleurisy
518	Other diseases of lung
519	Other diseases of respiratory system
530	Diseases of esophagus
536	Disorders of function of stomach
560	Intestinal obstruction without mention of hernia
562	Diverticula of intestine
569	Other disorders of intestine
571	Chronic liver disease and cirrhosis
572	Liver abscess and sequelae of chronic liver disease
577	Diseases of pancreas
578	Gastrointestinal hemorrhage
584	Acute renal failure
585	Chronic kidney disease (CKD)
599	Other disorders of urethra and urinary tract
600	Hyperplasia of prostate
682	Other cellulitis and abscess
707	Chronic ulcer of skin
724	Other and unspecified disorders of back
733	Other disorders of bone and cartilage
995	Certain adverse effects not elsewhere classified
996	Complications peculiar to certain specified procedures
997	Complications affecting specified body systems, not elsewhere classified
998	Other complications of procedures, NEC
E8798	Abn react-procedure NEC

References

[1] M. Abadi, A. Chu, I. Goodfellow, H.B. McMahan, I. Mironov, K. Talwar, L. Zhang, Deep learning with differential privacy, in: Proceedings of the 2016 ACM SIGSAC Conference on Computer and Communications Security, 2016, pp. 308–318.

[2] M. Artetxe, G. Labaka, E. Agirre. A robust self-learning method for fully unsupervised cross-lingual mappings of word embeddings, in: Proceedings of the 56th Annual Meeting of the Association for Computational Linguistics (Volume 1: Long Papers), Association for Computational Linguistics, Melbourne, Australia, 2018. pp. 789–798. doi:10.18653/v1/P18-1073.

[3] X. Bai, H. Cao, K. Chen, T. Zhao, A bilingual adversarial autoencoder for unsupervised bilingual lexicon induction, IEEE/ACM Transactions on Audio, Speech, and Language Processing 27 (2019) 1639–1648, https://doi.org/10.1109/TASLP.2019.2925973.

[4] J.S. Baik, Data privacy against innovation or against discrimination?: The case of the california consumer privacy act (ccpa), Telematics and Informatics 52 (2020).

[5] J. Baxter, Learning internal representations, in: Proceedings of the Eighth Annual Conference on Computational Learning Theory, 1995, pp. 311–320.

[6] Y. Bengio, L. Yao, G. Alain, P. Vincent, Generalized denoising auto-encoders as generative models, in: C.J.C. Burges, L. Bottou, M. Welling, Z. Ghahramani, K.Q. Weinberger (Eds.), Advances in Neural Information Processing Systems, Curran Associates Inc., 2013, pp. 899–907.

[7] Y.R. Chen, A. Rezapour, W.G. Tzeng, Privacy-preserving ridge regression on distributed data, Information Sciences 451–452 (2018) 34–49, https://doi.org/10.1016/j.ins.2018.03.061.

[8] E. Choi, M.T. Bahadori, E. Searles, C. Coffey, M. Thompson, J. Bost, J. Tejedor-Sojo, J. Sun, Multi-layer representation learning for medical concepts, in: Proceedings of the 22nd ACM SIGKDD International Conference on Knowledge Discovery and Data Mining, Association for Computing Machinery, New York, NY, USA, 2016, pp. 1495–1504, https://doi.org/10.1145/2939672.2939823.

[9] E. Choi, C. Xiao, W. Stewart, J. Sun. Mime: Multilevel medical embedding of electronic health records for predictive healthcare, in: S. Bengio, H. Wallach, H. Larochelle, K. Grauman, N. Cesa-Bianchi, R. Garnett (Eds.), Advances in Neural Information Processing Systems 31, 2018. pp. 4547–4557.

[10] Y. Choi, C.Y.I. Chiu, D. Sontag, Learning low-dimensional representations of medical concepts, AMIA Summits on Translational Science Proceedings 2016 (2016) 41.

[11] J. Choo, S. Bohn, G.C. Nakamura, A.M. White, H. Park, Heterogeneous data fusion via space alignment using nonmetric multidimensional scaling, in: Proceedings of the 2012 SIAM International Conference on Data Mining, SIAM, 2012, pp. 177–188, https://doi.org/10.1137/1.9781611972825.16.

[12] J. Devlin, M.W. Chang, K. Lee, K. Toutanova. BERT: Pre-training of deep bidirectional transformers for language understanding, in: Proceedings of the 2019 Conference of the North American Chapter of the Association for Computational Linguistics: Human Language Technologies, Volume 1 (Long and Short Papers), Association for Computational Linguistics, Minneapolis, Minnesota, 2019. pp. 4171–4186. doi:10.18653/v1/N19-1423.

[13] C. Dwork, Differential privacy: A survey of results, in: M. Agrawal, D. Du, Z. Duan, A. Li (Eds.), Theory and Applications of Models of Computation, Springer Berlin Heidelberg, Berlin, Heidelberg, 2008, pp. 1–19.

[14] W. Farhan, Z. Wang, Y. Huang, S. Wang, F. Wang, X. Jiang, A predictive model for medical events based on contextual embedding of temporal sequences, JMIR Medical Informatics 4 (2016) e39, https://doi.org/10.2196/medinform.5977.

[15] C. zhi Gao, Q. Cheng, P. He, W. Susilo, J. Li. Privacy-preserving naive bayes classifiers secure against the substitution-then-comparison attack, Information Sciences 444 (2018) 72–88. doi:https://doi.org/10.1016/j.ins.2018.02.058.

[16] J.C. Gower, Generalized procrustes analysis, Psychometrika 40 (1975) 33–51.

[17] Y. Huang, J. Lee, S. Wang, J. Sun, H. Liu, X. Jiang, Privacy-preserving predictive modeling: Harmonization of contextual embeddings from different sources, JMIR Medical Informatics 6 (2018) e33, https://doi.org/10.2196/medinform.9455.

[18] D. Ienco, R.G. Pensa, Enhancing graph-based semisupervised learning via knowledge-aware data embedding, IEEE Transactions on Neural Networks and Learning Systems 31 (2020) 5014–5020, https://doi.org/10.1109/TNNLS.2019.2955565.

[19] H. Jia, S. Ding, M. Du, Y. Xue, Approximate normalized cuts without eigen-decomposition, Information Sciences 374 (2016) 135–150, https://doi.org/10.1016/j.ins.2016.09.032.

[20] A.E. Johnson, T.J. Pollard, L. Shen, H.L. Li-Wei, M. Feng, M. Ghassemi, B. Moody, P. Szolovits, L.A. Celi, R.G. Mark, Mimic-iii, a freely accessible critical care database, Scientific Data 3 (2016) 1–9.

[21] M. Kim, J. Lee, L. Ohno-Machado, X. Jiang, Secure and differentially private logistic regression for horizontally distributed data, IEEE Transactions on Information Forensics and Security 15 (2020) 695–710.

[22] M. Kim, Y. Song, S. Wang, Y. Xia, X. Jiang, Secure logistic regression based on homomorphic encryption: Design and evaluation, JMIR Medical Informatics 6 (2018) e19, https://doi.org/10.2196/medinform.8805.

[23] A.Y. Lau, P. Staccini, et al, Artificial intelligence in health: New opportunities, challenges, and practical implications: Findings from the yearbook 2019 section on education and consumer health informatics, Yearbook of Medical Informatics 28 (2019) 174.

[24] J. Lee, W. Lee, I.S. Park, H.S. Kim, H. Lee, C.H. Jun, Risk assessment for hypertension and hypertension complications incidences using a bayesian network, IIE Transactions on Healthcare Systems Engineering 6 (2016) 246–259, https://doi.org/10.1080/19488300.2016.1232767.

[25] J. Lee, J. Sun, F. Wang, S. Wang, C.H. Jun, X. Jiang, Privacy-preserving patient similarity learning in a federated environment: Development and analysis, JMIR Medical Informatics 6 (2018) e20, https://doi.org/10.2196/medinform.7744.

[26] S.D. Lee, J.H. Lee, Y.G. Choi, H.C. You, J.H. Kang, C.H. Jun, Machine learning models based on the dimensionality reduction of standard automated perimetry data for glaucoma diagnosis, Artificial Intelligence in Medicine 94 (2019) 110–116.

[27] X. Li, J. She, Collaborative variational autoencoder for recommender systems, in: Proceedings of the 23rd ACM SIGKDD International Conference on Knowledge Discovery and Data Mining, Association for Computing Machinery, New York, NY, USA, 2017, pp. 305–314, https://doi.org/10.1145/3097983.3098077.

[28] Y. Li, X. Jiang, S. Wang, H. Xiong, L. Ohno-Machado, VERTIcal Grid lOgistic regression (VERTIGO), Journal of the American Medical Informatics Association 23 (2015) 570–579, https://doi.org/10.1093/jamia/ocv146.

[29] Z. Li, K. Roberts, X. Jiang, Q. Long, Distributed learning from multiple ehr databases: Contextual embedding models for medical events, Journal of Biomedical Informatics 92 (2019) 103138.

[30] Y. Liu, Z. Xu, C. Li, Distributed online semi-supervised support vector machine, Information Sciences 466 (2018) 236–257, https://doi.org/10.1016/j.ins.2018.07.045.

[31] X. Ma, F. Zhang, X. Chen, J. Shen, Privacy preserving multi-party computation delegation for deep learning in cloud computing, Information Sciences 459 (2018) 103–116, https://doi.org/10.1016/j.ins.2018.05.005.

[32] Z. Ma, J. Ma, Y. Miao, X. Liu, Privacy-preserving and high-accurate outsourced disease predictor on random forest, Information Sciences 496 (2019) 225–241, https://doi.org/10.1016/j.ins.2019.05.025.

[33] M.T. Mardini, Z.W. Ras, Extraction of actionable knowledge to reduce hospital readmissions through patients personalization, Information Sciences 485 (2019) 1–17, https://doi.org/10.1016/j.ins.2019.02.006.

[34] B. McMahan, E. Moore, D. Ramage, S. Hampson, B.A. y Arcas, Communication-efficient learning of deep networks from decentralized data, in: A. Singh, J. Zhu (Eds.), Artificial Intelligence and Statistics, PMLR, Fort Lauderdale, FL, USA, 2017, pp. 1273–1282.

[35] L. Melis, C. Song, E. De Cristofaro, V. Shmatikov. Exploiting unintended feature leakage in collaborative learning, in: 2019 IEEE Symposium on Security and Privacy (SP), 2019, pp. 691–706.

[36] T. Mikolov, K. Chen, G. Corrado, J. Dean. Efficient estimation of word representations in vector space, arXiv preprint arXiv:1301.3781 (2013).

[37] R. Nosowsky, T.J. Giordano. The health insurance portability and accountability act of 1996 (hipaa) privacy rule: Implications for clinical research, Annual Review of Medicine 57 (2006) 575–590. doi:10.1146/annurev.med.57.121304.131257.

[38] S.M. Nurmi, M. Kangasniemi, A. Halkoaho, A.M. Pietilä, Privacy of clinical research subjects: An integrative literature review, Journal of Empirical Research on Human Research Ethics 14 (2019) 33–48, https://doi.org/10.1177/1556264618805643.

[39] J. Pennington, R. Socher, C.D. Manning, Glove: Global vectors for word representation, in: Proceedings of the 2014 Conference on Empirical Methods in Natural Language Processing (EMNLP), 2014, pp. 1532–1543.
[40] A. Ranjan, T. Bolkart, S. Sanyal, M.J. Black, Generating 3d faces using convolutional mesh autoencoders, in: Proceedings of the European Conference on Computer Vision (ECCV), 2018, pp. 704–720.
[41] D.J. Rezende, S. Mohamed, D. Wierstra. Stochastic backpropagation and approximate inference in deep generative models, in: Proceedings of the 31st International Conference on Machine Learning – Volume 32, JMLR.org, 2014, pp. 1278–1286.
[42] A.P. Sarath Chandar, S. Lauly, H. Larochelle, M. Khapra, B. Ravindran, V.C. Raykar, A. Saha. An autoencoder approach to learning bilingual word representations, in: Z. Ghahramani, M. Welling, C. Cortes, N.D. Lawrence, K.Q. Weinberger (Eds.), Advances in Neural Information Processing Systems 27, Curran Associates Inc, 2014, pp. 1853–1861.
[43] B. Shickel, P.J. Tighe, A. Bihorac, P. Rashidi, Deep ehr: A survey of recent advances in deep learning techniques for electronic health record (ehr) analysis, IEEE Journal of Biomedical and Health Informatics 22 (2018) 1589–1604, https://doi.org/10.1109/JBHI.2017.2767063.
[44] J. Su, S. Wu, B. Zhang, C. Wu, Y. Qin, D. Xiong, A neural generative autoencoder for bilingual word embeddings, Information Sciences 424 (2018) 287–300, https://doi.org/10.1016/j.ins.2017.09.070.
[45] P. Voigt, A. Von dem Bussche, The Eu General Data Protection Regulation (gdpr). A Practical Guide, first ed., Springer International Publishing, Cham, 2017.
[46] F. Wang, A. Preininger, Ai in health: State of the art, challenges, and future directions, Yearbook of Medical Informatics 28 (2019) 16.
[47] X. Zhang, C. Liu, S. Nepal, C. Yang, W. Dou, J. Chen. Combining top-down and bottom-up: Scalable sub-tree anonymization over big data using mapreduce on cloud, in: 2013 12th IEEE International Conference on Trust, Security and Privacy in Computing and Communications, 2013, pp. 501–508.
[48] D. Zhu, H. Zhu, X. Liu, H. Li, F. Wang, H. Li, D. Feng, Credo: Efficient and privacy-preserving multi-level medical pre-diagnosis based on ml-knn, Information Sciences 514 (2020) 244–262, https://doi.org/10.1016/j.ins.2019.11.041.
[49] L. Zhu, Z. Liu, S. Han, Deep leakage from gradients, in: Advances in Neural Information Processing Systems 32, 2019, pp. 14774–14784.